[redacted]

Carbon Capture from Gaseous Landfill Emissions
Part 1: CO_2 Capture from Landfill Gas

Date of Submission (1/2020)

Umadevi Gopalakrishnan, Olusola Isaac Johnson, Madeline Van Dyne, Yetunde Oluwatosin Sokefun, Babu Joseph (co-PI), and John N. Kuhn (PI)

Hinkley Center for Solid and Hazardous Waste Management
University of Florida
P. O. Box 116016
Gainesville, FL 32611
www.hinkleycenter.org

Report #

Acknowledgments

The authors gratefully acknowledge funding from Hinkley Center for Solid and Hazardous Waste Management. In addition, financial support from the College of Engineering at the University of South Florida is greatly appreciated. We also thank our Technical Awareness Group (TAG) for the time and efforts on this project.

TABLE OF CONTENTS

LIST OF FIGURES

List of Tables

List of Abbreviations & Acronyms

i. Compressed Natural Gas	CNG
ii. Water Scrubbing	WS
iii. Chemical Scrubbing	CS
iv. Pressure Swing Adsorption	PSA
v. Aminopropyltriethoxysilane	APTES
vi. Landfill Gas	LFG
vii. Municipal Solid Waste	MSW
viii. Gallon Gasoline Equivalent	GGE
ix. Annual Growth Rate	AGR
x. Organic Physical Scrubbing	OPS
xi. Ethylenediaminetetraacetic acid)	EDTA
xii. Membrane Separation	MS
xiii. Temperature Swing Adsorption	TSA
xiv. Poly(ethylenimine)	PEI
xv. Poly(allylamine)	PAA
xvi. Monoethanolamine	MEA
xvii. Diethanolamine	DEA
xviii. X-ray diffraction	XRD
xix. Fourier-Transform Infrared Spectroscopy	FTIR
xx. Temperature Programmed Oxidation	TPO
xxi. Brunauer -Emmett-Teller	BET
xxiii. Barrett-Joyner-Halenda	BJH
xxiv. Attenuated Total Reflection	ATR
xv. Tetraethylenepentamine	TEPA
xvi. Supported Amine Sorbent	SAS

ABSTRACT

Biogas, being rich in methane, can be used as a fuel for various end uses such as electricity generation, compressed natural gas (CNG), production of liquid fuels, industrial heating, etc. CO_2 is the major contaminant in biogas (30-50%) along with other impurities such as NH_3, H_2S, and water. CO_2 in the biogas decreases the heating value of biogas. Natural gas pipelines and vehicle use require high purity (> 95%) CH_4. There are many commercial techniques available for CO_2 removal from biogas such as water scrubbing (WS), chemical scrubbing (CS) using amine solutions, and pressure swing adsorption (PSA). These techniques have disadvantages including corrosion problems in pipelines, heavy use of water, and high energy requirement in the regeneration step and/or drying steps. CO_2 adsorption using amine-functionalized silica is a low-pressure process and can reduce the capital and operating expenses of compressors required in biogas upgrading.

In the work reported here, APTES was immobilized on mesoporous SBA-15. It was prepared using conventional grafting techniques. Techniques including XRD, N_2 physisorption, FTIR and TPO were used for sample characterization. A series of APTES modified SBA-15 were tested for adsorption experiments of CO_2 at room temperature and 1 atm for a dry 50% CO_2 in He feeds. Results show that with an increase in APTES loading from 12 to 26 wt% APTES the CO_2 adsorption capacity increases from 0.069 mmol/g to 0.85 mmol/g. The presence of water did not affect the CO_2 adsorption capacity; however, water adsorption increases with an increase in water concentration in the feed as silica is capable of water adsorption independently of the grafted moieties. The results suggest that the adsorption of water and CO_2 is happening in two different sites because of which CO_2 adsorption remains constant even when water concentration in the feed increases. Regeneration study in the presence of water showed almost constant CO_2 adsorption capacity for 5 cycles. CO_2/CH_4 adsorption study in He and dry CO_2/CH_4 feed-in 1:1 ratio showed that the sample has a high affinity to CO_2. Also, the adsorption capacity of CO_2 does not change in the presence of CH_4. The adsorbents showed a decrease of 30% in adsorption capacity (0.50 mmol/g) when landfill gas was used as feed because of site blocking by impurities present in biogas. However, consistent CO_2 adsorption capacities were obtained for five regeneration cycles.

The techno-economic and sensitivity analyses for the CO_2 separation from biogas with amine-functionalized silica sorbents were also completed. The economic performance is compared to conventional biogas upgrading technologies. As the basis of the analysis, 1000 SCFM of biogas with a 60/40 percent volume of CH_4/CO_2 is to be upgraded to a gas stream with a purity of 97%+ methane. The cost of upgrading using the amine-functionalized silica decrease with increasing plant capacity. The cost associated with the amine-modified silica represents the least capital and operating investment in comparison to current biogas upgrading technologies. From the study, APTES modified silica adsorbents are promising for the removal of CO_2 and H_2O simultaneously from biogas.

KEYWORDS: Biogas, CO_2 adsorption, APTES modified SBA 15

1. INTRODUCTION AND BACKGROUND

1.1 Motivation

For many years, we have relied on fossil fuel as the major source of energy but today use of oil, coal, and gas has become a major concern due to the buildup of CO_2 in the atmosphere and its impact on climate. Combustion of fossil fuels results in the emission of greenhouse gases, considered to be a major contributor to drastic changes in the global climate. Also, fossil fuels are a finite source of energy and they will eventually become too scarce or very hard to retrieve. With the increase in population, increasing economic growth and rising standards of living there is increased energy consumption. So, for the growing energy demand, we need an energy consumption plan which is sustainable.

Recovering energy from waste is one of the avenues available for renewable energy production. According to the US EPA, about 234 million metric tons were generated in the US in 2016 (Lee *et al* 2017). Over the years many investments have been made by waste managers around the world to reuse the waste – by recycling or by converting it into energy. Landfill gas (LFG) coming from the municipal solid waste (MSW) disposal sites contains about 50 percent methane and is potentially a renewable energy source. The LFG generated from 1 million tons of MSW can be used to produce around 0.78 MW of electricity or nearly half a million gallons of gasoline equivalent (GGEs) per year (EPA 2016).

LFG is generated from landfills by the anaerobic digestion of the biodegradable portion of the MSW by microorganisms. The biomass in MSW is broken down using natural processes like acetogenesis and methanogenesis to produce landfill gas which consists of approximately 50% CH_4 and 50 % CO_2. LFG also contains other compounds in lesser amounts, including hazardous air pollutants and VOCs, which can create health hazards. Methane is a potent greenhouse gas and uncollected methane can lead to fire and explosion. So, for larger landfills, the EPA requires landfill operators to regularly monitor and treat LFG emissions. Methane emissions from the landfills account for more than 15 percent of US methane emissions in 2015 (EPA 2016). Even today, with the modern well-coordinated waste to energy facilities, most of the carbon from the carbon-containing products that come out from the landfill are combusted/flared for energy ultimately for the final product to be CO_2. According to the Environmental Protection Agency (EPA) (LMOP 2019), as of 2015 the EPA is tracking 619 LFG projects that are operational today which generates 2044 MW of electricity and 342 MMSCFD of gas for other uses. Also, there are about 480 candidate landfills which will add 900 MW of electricity and 500 MMSCFD to the current capacity (EPA 2019).

LFG has an energy content of 450-600 BTU/ft^3 and because of this high energy content, many efforts have been made to capture the methane and use it as a resource. The methane from LFG can be used for various end uses such as electricity generation, compressed natural gas (CNG) production, gasoline/diesel fuel production, industrial heating, etc. However, to increase the calorific value of the LFG and use this energy content the LFG needs to be cleaned or upgraded. CO_2 being the major contaminant its removal from methane becomes one of the critical steps in

biogas upgrading. The increase in the biogas upgrading units every year shows that there is an increasing interest in use of this technology (Bauer *et al* 2013). According to the Global Market Outlook (2017-2026), $0.62 billion was accounted by the biogas upgrading market in 2017 and by 2026 is expected to reach a total of $4.6 billion growing at a compound annual growth rate (CAGR) of 26% (Jang *et al* 2018). The market growth is influenced by some key factors such as increasing demand for renewable energy, demand for waste treatment, push for the reduction of greenhouse gases and strict policies and regulation from the government (Jang *et al* 2018). Due to stringent purity specifications, production of compressed natural gas (CNG) and pipeline quality natural gas have high costs of purification associated with it. The main goal of this project is to develop efficient, low-cost adsorbents for CO_2 removal from biogas.

1.2 Landfill Gas Purification

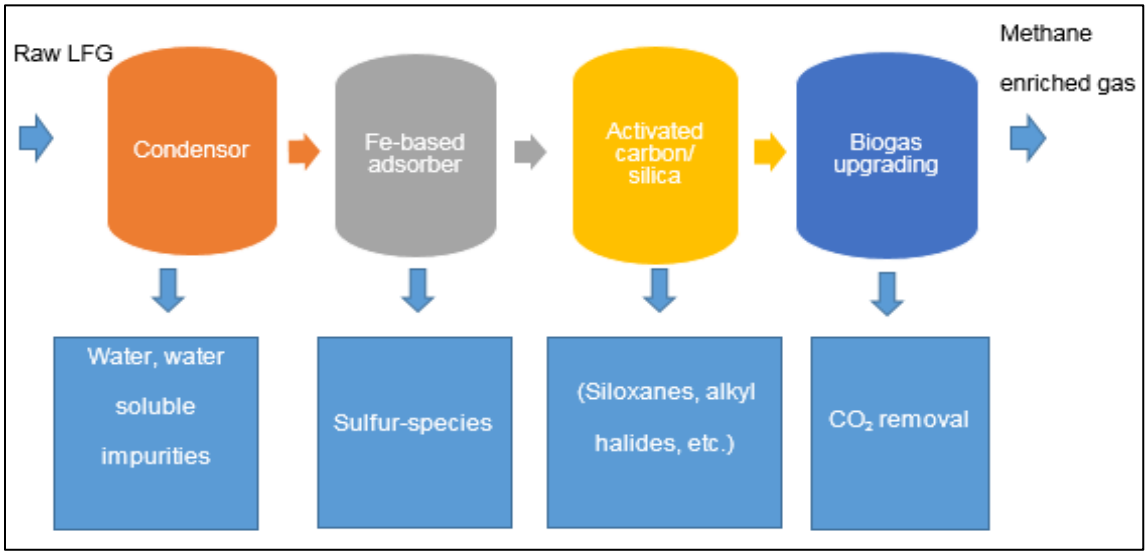

Figure 1. LFG purification process to produce methane enriched gas

In the overall biogas clean-up process shown in Figure 1, the first treatment is focused mainly on removal of H_2S along with other impurities like VOCs, siloxanes, CO, and NH_3. The second step is the biogas upgrading for removing CO_2 and purifying the gas to specifications similar to natural gas. Purity of >95 % CH_4 may be required depending on regulations and specifications.

H_2S from the biogas is usually removed before CO_2 removal because it can adversely affect downstream processing. Even though H_2S concentration in the biogas is very low, it can easily get converted to sulfuric acid (H_2SO_4) and sulfur dioxide (SO_2) which are highly corrosive to pipelines. Techniques including chemical absorption, adsorption using activated carbon, and chemical/aqueous scrubbing are used for H_2S removal. H_2S can also poison catalysts used in downstream processing.

The number of biogas upgrading units have been increasing every year. In Europe for example, over the years 2001 to 2011 biogas upgrading unit capacities grew from 10,000 N m^3/h (raw gas) to over 160,000 N m^3/h (raw gas), respectively (Sun *et al* 2015). By 2030, use of upgraded biomethane as biofuel and for grid injections can reach up to 18-20 billion Nm^3 (Scarlat *et al* 2018, Scarlat *et al* 2015). There is a clear interest to study biogas upgrading techniques. There are various technologies developed for biogas upgrading process including water scrubbing (WS), pressure swing adsorption (PSA), membrane separation (MS), and cryogenic separation among others. The distribution of biogas upgrading technologies currently in use is shown in Figure 2.

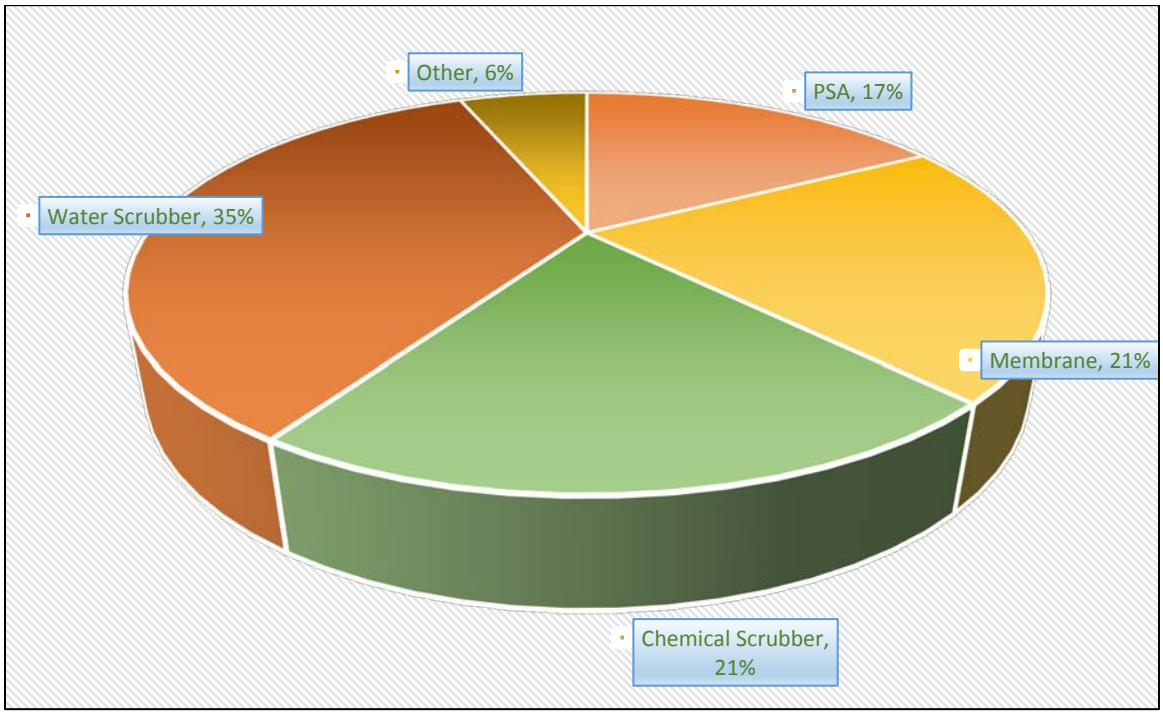

Figure 2. Types of biogas upgrading technology in use currently. Adapted from IEA Bioenergy Task 37 and European Biogas Association (Hoyer *et al* 2016)

Pressure swing adsorption (PSA) uses adsorbent materials such as modified activated carbon, silica gel, and zeolites to selectively adsorb CO_2 onto solid surfaces based on their molecular structure (F. Bauer 2013). CO_2 preferentially adsorbs on these materials and this difference is exploited in the separation process. H_2S can also be removed using this process using appropriate adsorbents but usually H_2S is removed before it is sent to a PSA unit. Pretreatment is recommended as the H_2S and other impurities can easily foul the adsorbents. The major cost of PSA is associated with the capital and operating costs of the compressors used. Typically, adsorption is carried out at 3-8 bar and desorption at 0.1-0.2 bar. Another alternative is to use temperature swing adsorption (TSA) to reduce operational costs. Adsorption in a TSA process is carried out in a temperature range of 50-60 °C at constant pressure and the regeneration of the adsorbent is done at a higher temperature.

Membrane separation uses molecular sieves for selective permeation of different gases based on the difference in their size and chemical affinity (Sahota *et al* 2018). Highly soluble smaller molecules including CO_2 and H_2S preferentially pass through the membrane when there is a pressure difference or a concentration gradient across the membrane. High membrane costs and low stability of membranes are a major challenge.

Water scrubbing uses the solubility property of gases. CO_2 has a higher solubility than CH_4 in water at 25 °C. This process is usually carried out in a pressure range of 6-10 bar. Water scrubbing corresponds to 41% of the total biogas upgrading market because of its low cost, easy availability, low/no use of chemicals and low sensitivity to other impurities present in biogas (Awe *et al* 2017, Kadam and Panwar 2017). Another challenge is the gas usually must be dried twice, with some drying occurring before compression and then again after the separation depending on the next unit process.

Chemical scrubbing typically uses aqueous amine solutions to dissolve CO_2. Aqueous amine solutions are highly selective to CO_2 and other gases like CH_4, N_2 and O_2 are not absorbed. The absorption is usually done at T = 20-40 $^{\circ}$C and P = 1-2 bar. The stripping step is carried out at higher temperatures of up to 120-150 $^{\circ}$C using steam in an operating pressure of 1.5-3 bar (Hjuler and Aryal 2017). Use of solvents has the disadvantages of heavy usage of solvents, corrosion problems in pipelines, and high energy consumption during regeneration and treatment of the chemical waste generated.

Because of the high capital and operating costs of these commercially available technologies for biogas upgrading, many alternative techniques are being studied. Adsorption of CO_2 on solid sorbents are gaining interest because of their high selectivity, easy regeneration and less energy usage. Solid adsorbents like activated carbons, metal oxides, hydrotalcites, metal organic frameworks and mesoporous silica have been developed as an alternative CO_2 capture technology. Among these, surface modified mesoporous silica sorbents using amine functionalization groups because of their high selectivity, easy regeneration, and stability are promising candidates for biogas upgrading process. Figure 3 shows CO_2 removal process using solid adsorbents.

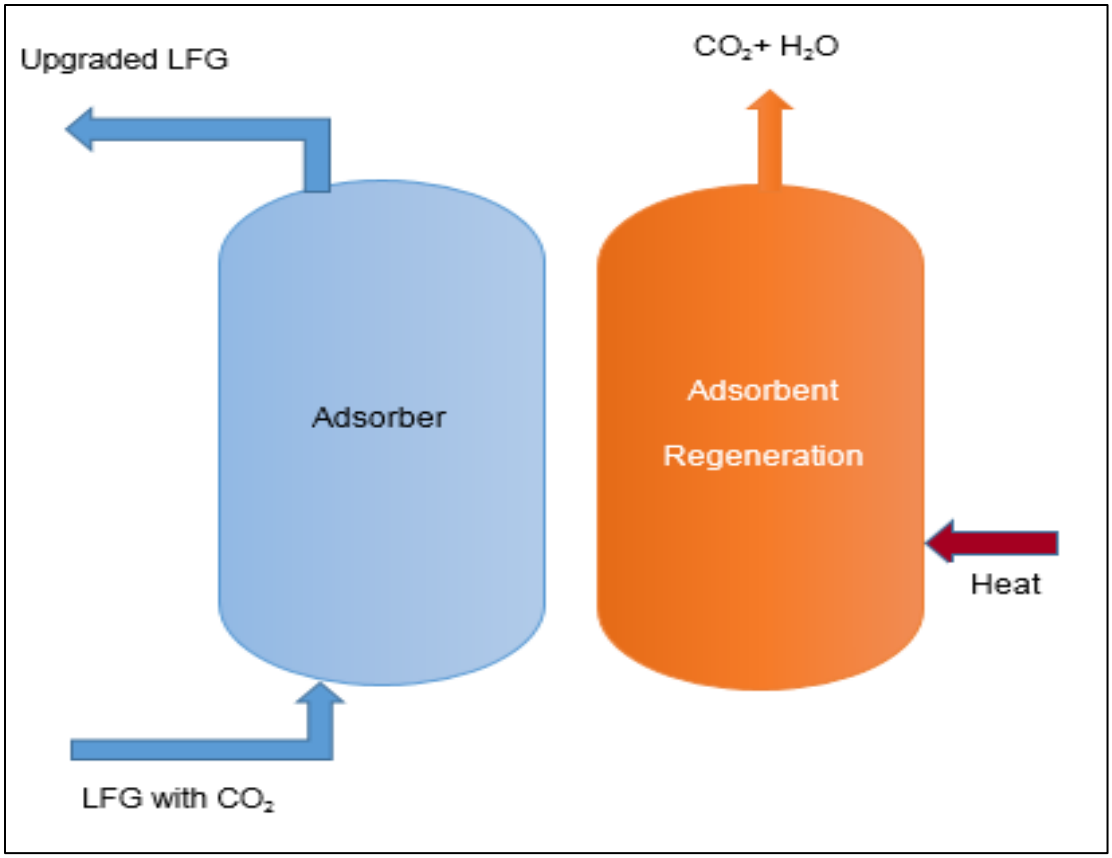

Figure 3. CO_2 removal using adsorbents. Adapted from Sutanto et al.(Sutanto *et al* 2017b)

Amine sorbents can be classified into 3 categories. Category 1 solid sorbents consist of physically loaded or impregnated polymeric/monomeric amine on a porous support. Category 2 sorbents consist of covalently grafted amine groups like amino silanes to mesoporous silica. Category 3, a hybrid of the other two categories consists of amino polymers which have been polymerized in situ on porous supports. Examples of category 1 are poly(ethylenimine) (PEI) and poly(allylamine) (PAA). Aminopropyltriethoxysilane (APTES) is an example of category 2 sorbent (see Figure 4). Some of the important factors to be considered while choosing the support is the adsorption capacity of CO_2, selectivity towards CO_2, ease of regeneration and stability of the support, tolerance to impurities, and costs. Sorbent costs should be in the range of $5-10/kg of sorbent, anything above $15/kg is not considered economical (Shi *et al* 2017).

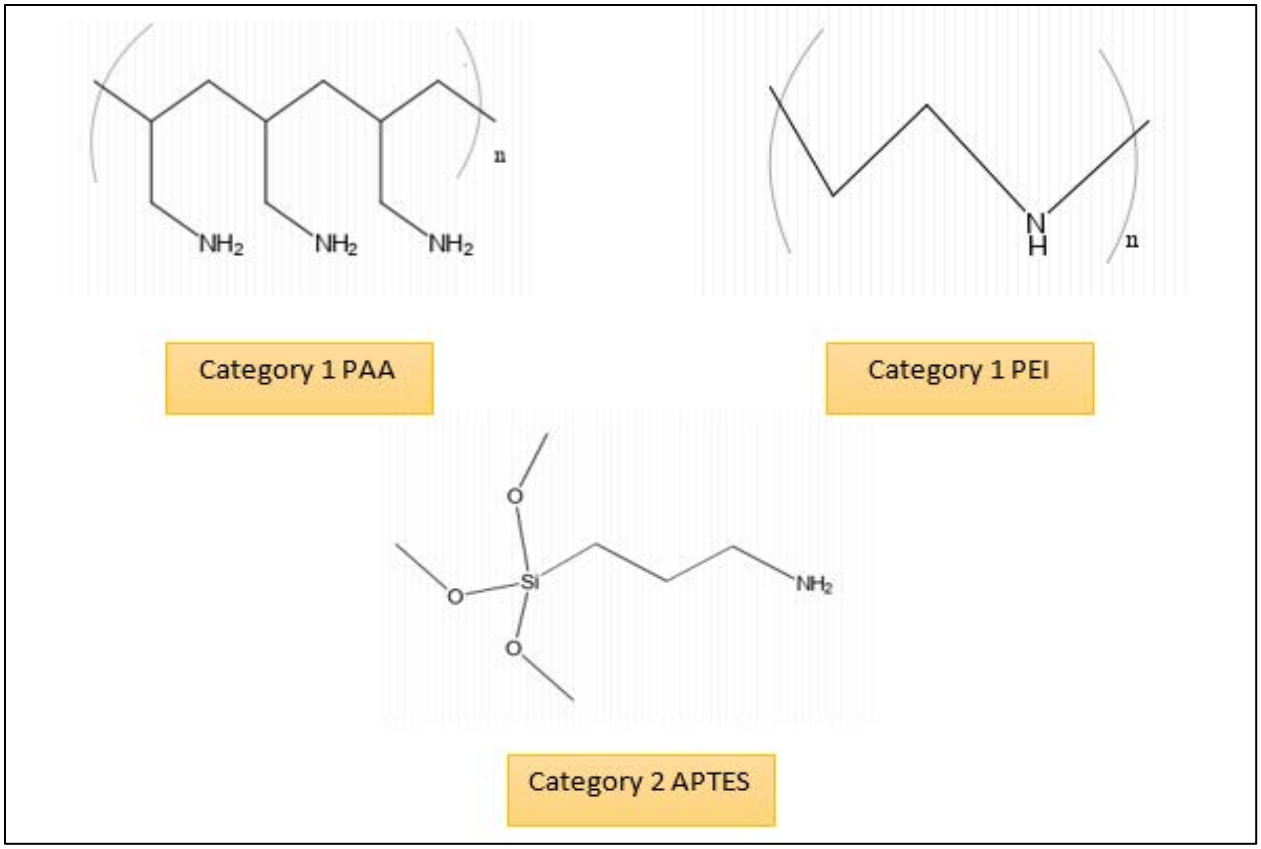

Figure 4. Examples of category 1 and category 2 sorbents. Category 1 amine groups are physically loaded on the support and in category 2, the amine groups are covalently grafted on the support silica.

Use of an amine-based adsorbent for CO_2 removal has a mechanism similar to the one used in the chemical scrubbing processes. Using solids instead of solvents has many advantages in terms of their heat capacity and reduced energy requirement during regeneration. Some of the common amine solvents used commercially such as MEA (monoethanolamine), and DEA (diethanolamine) has been explored as solid adsorbents for CO_2 removal (Lara *et al* 2018). Adsorption capacities from 0.23 mmol/g to 3.18 mmol/g have been reported (Lara *et al* 2018). In comparison, the adsorption capacity in a CS process using MEA is about 0.01 mmol/g MEA (Budzianowski 2012). Thus, solid sorbents are promising for biogas upgrading and can play an important role in reducing energy requirements, increasing CO_2 capture efficiency and decreasing regeneration energy requirements (Lara *et al* 2018).

1.3 Objectives of This Study

The main objective of the work was to evaluate the use of amine-functionalized silica sorbent for biogas upgrading. We will focus on APTES functionalized silica for this study. Specific objectives are to determine the optimum loading for maximum adsorption of CO_2 in CO_2/CH_4 gas mixtures and to determine the CO_2 adsorption capacity of the adsorbents in pure CO_2 and CO_2/CH_4 mixtures in dry and humid conditions. CO_2 isotherms for the different samples at room temperature will be measured. Selectivity of the adsorbent in CO_2/CH_4 gas mixture also will be evaluated. The effect of water on the adsorption capacity and stability will also be investigated. To determine the regeneration and stability of the adsorbent, multiple adsorption cycles will be carried out. Finally, CO_2 adsorption using real landfill gas will be evaluated.

1.4 Scope of Work

This work will focus on only one adsorbent: namely, APTES functionalized on SBA-15. For a brief period of time, EDTA (ethylenediaminetetraacetic acid) functionalized SBA-15 was studied for CO_2 removal. Since it had a poor adsorption capacity, it was not explored further. Results of the same are summarized in Appendix A. There are many other possibilities also but that is left as future work. We will consider the effect of loadings, CO_2 adsorption capacity, regeneration ability and tolerance of the adsorbent to water and methane in the feed gas. In addition, we will also explore the effect of other impurities namely present in LFG.

2. BACKGROUND

Landfill gas contains mainly CH_4 and CO_2 in addition to small amounts of impurities like hydrogen sulfide (H_2S), ammonia (NH_3), oxygen (O_2), nitrogen (N_2), hydrogen (H_2), water and carbon monoxide (CO). Detailed composition of typical LFG along with a comparison to natural gas is shown in Table 1 (Sun *et al* 2015). Typical specifications of the gas for injecting it into natural gas grids are also included in the table. In order to upgrade the biogas to a higher fuel standard it is important to reduce the impurities like CO_2 and H_2S in the LFG. These impurities can cause corrosion in pipelines, damage due to the formation of ice and condensate, poisoning of the catalytic converter and the release of harmful emissions. CO_2 must be removed to increase the heating value of the gas and to meet pipeline gas quality specifications.

Table 1. Comparison between LFG and natural gas compositions

Parameter	**Unit**	**Landfill Gas**	**Biogas (AEBIOM 2012)**	**Natural Gas at source (Sun *et al* 2015)**	**Natural gas grid injection specifications (Mokhatab *et al* 2019)**
Lower heating Value	MJ/Nm^3	16	23	40	
	kWh/Nm^3	4.4	6.5	11	
	MJ/Kg	12.3	20.2	47	
Density	Kg/Nm^3	1.3	1.2	0.8	
Higher Wobble Index	MJ/Nm^3	18	27	51	
CH_4	vol-%	35-65	50-75	85-92	70-98
CO_2	vol-%	15-40	25-45	0.2-1.5	2-4
H_2O	lbm H_2O/MMscf gas	1-5	1-2	-	4-7

Table 1. Comparison between LFG and natural gas compositions (Cont.)

Parameter	**Unit**	**Landfill Gas**	**Biogas (AEBIOM 2012)**	**Natural Gas at source (Sun *et al* 2015)**	**Natural gas grid injection specifications (Mokhatab *et al* 2019)**
N_2	vol-%	15	1-5	0.3	4-5
O_2	vol-%	1	Trace	-	0.01
H_2S		0-100 ppm	0.1-0.5	1.1-5.9 ppm	0.25– 1.0 grain/100 scf
NH_3	ppm	5 ppm		-	-
H_2	vol-%	0-3	0-3	-	-

As mentioned before, there are many commercially available technologies for gas purification but the challenges lie in the high costs of operation and heat/energy/water requirements (Ullah Khan *et al* 2017). The capital and operating costs of these systems depends on many factors such as type of technology used, plant capacity, methane purity required, and raw biogas quality (Ullah Khan *et al* 2017). Figure 5 shows the capital costs for PSA, WS, organic physical scrubbing (OPS), and CS as a function of capacity. The source data was collected in the year 2009.

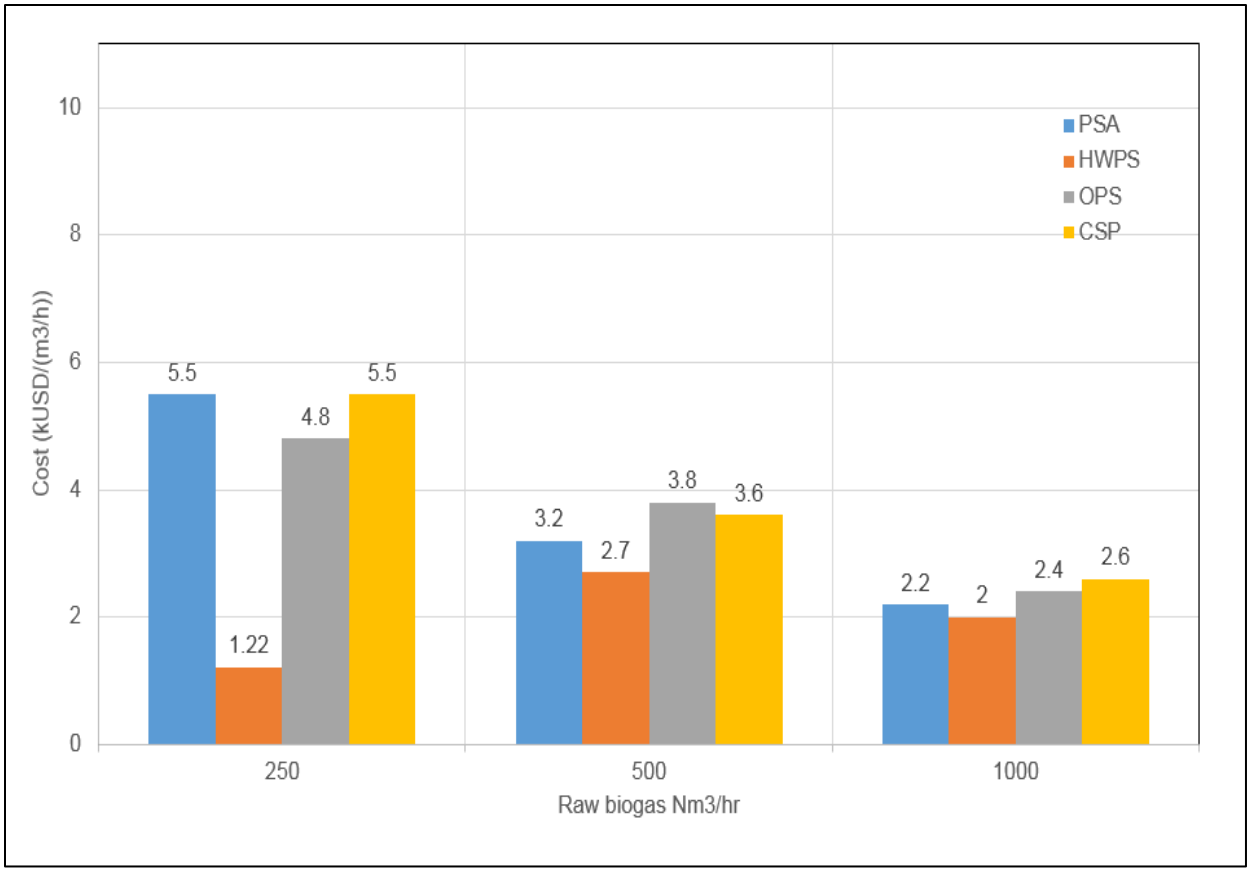

Figure 5. Capital costs of biogas upgrading technologies for different plant capacities. Adapted from Khan(Ullah Khan *et al* 2017)

Costs decrease with increase in pant capacity due to economy of scale. At higher flow rates the plant capital costs are similar, but CS has significantly lower capital costs. On comparing the total costs (Figure 6) which includes operating and maintenance costs of biogas upgrading, chemical scrubbing has the lowest cost at lower flow rates and water scrubbing has the highest. However, at higher flow rates, all the units have similar costs and there is no clear winner. The source data was collected in the year 2007-2008.

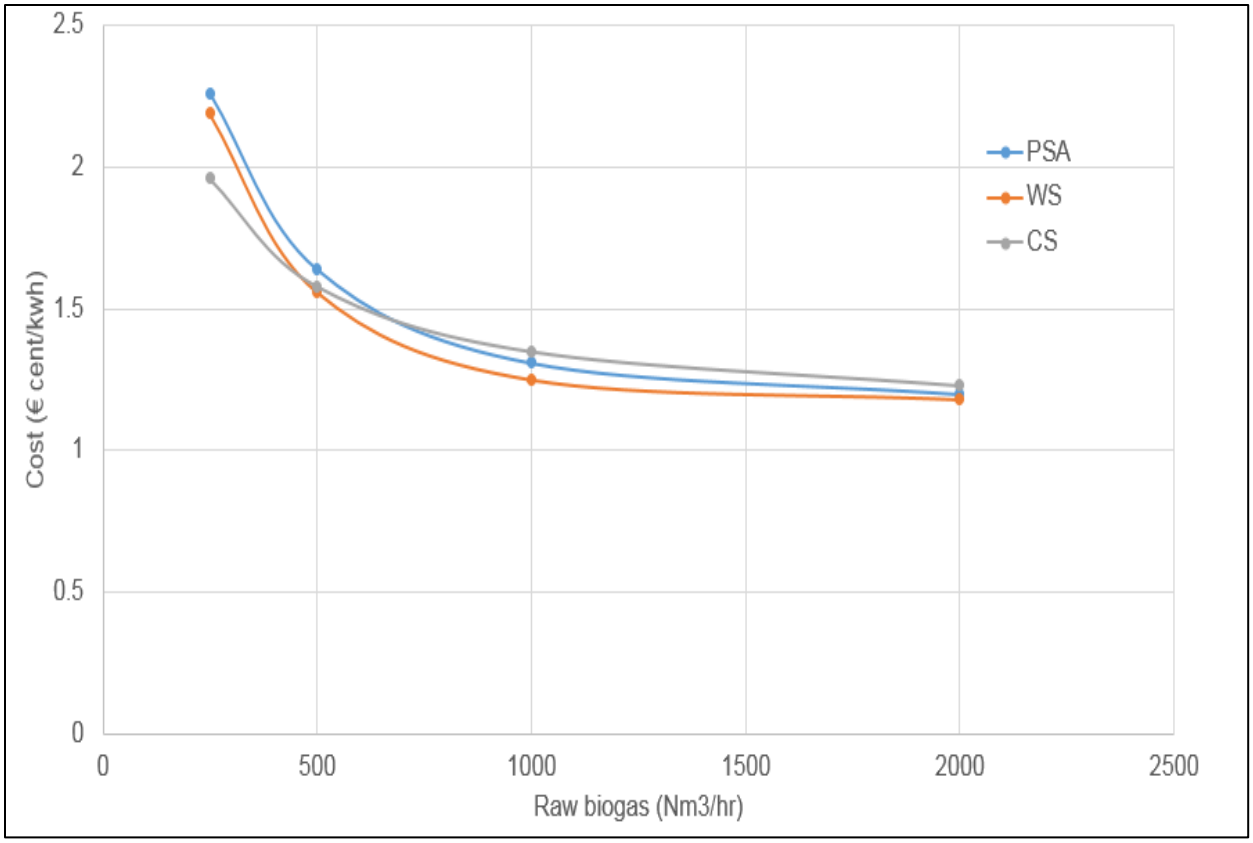

Figure 6. Cost of biogas upgrading units. Adapted from Warren (Warren 2012)

Table 2. Comparing and contrasting biogas upgrading technologies. From ref (Sun *et al* 2015, Yang *et al* 2014)

CO_2 removal approaches	Advantages	Limitations
Pressure Swing Adsorption (PSA)	Low CH_4 slip No use of chemicals	Prior water and H_2S removal required Low emissions
Water Scrubbing (WS)	Low CH_4 slip	Pre separation of H_2S required High water and energy demand
Chemical Scrubbing (CS)	Low methane slip Efficient H_2S removal	Expensive High energy requirement Corrosion
Membrane Separations (MS)	Less energy demands	High CH_4 slip at higher purity Can be expensive
Organic physical scrubbing (OPS)	Low temperature CH_4 purity up to 98%	High pressure Prior separation of H_2S and NH_3 required

Use of solid amine sorbents can decrease the sensible heat requirement and can lower corrosion problems as the amine groups are grafted on a solid support (Sutanto *et al* 2017b). In fact, compared to the commercially available amine scrubbing process, the energy requirement for amine grafted sorbents is smaller and estimated to be only 4.2-4.6 GJ/ton CO_2 whereas for amine scrubbing process it is 7.5 GJ/ton CO_2 (Sutanto *et al* 2017b). Also, specific relative primary energy requirement is 20-22% smaller for solid amine adsorbent units than amine scrubbing process. Amine groups have strong affinity to CO_2 so adsorption can be carried out at low pressures, which can lower compressor costs. Compressor costs can add up significantly to the total costs (Kent 2016).

There have been many studies on the use of solid amine supports for CO_2 removal from air (Belmabkhout *et al* 2010b, Choi *et al* 2009, Eisenberger *et al* 2009). However, there are fewer studies on amine functionalized supports for CO_2 removal from biogas where the concentration of CO_2 is much higher (Belmabkhout *et al* 2009a, Quan *et al* 2017, Sutanto *et al* 2017b, Zhou *et al* 2017). Initial studies on CO_2 adsorption from a pure and binary CO_2/CH_4 mixture using just MCM-

41 without any amine loading showed higher adsorption capacity in a high pressure PSA process (Belmabkhout and Sayari 2009, Belmabkhout *et al* 2009b). This value was higher than NoritAC (activated carbon) which is a very well-known adsorbent for PSA process (Belmabkhout and Sayari 2009). CO_2/CH_4 separation using TRI_PE MCM (Trimethoxy silylpropyl amino (pore expanded) ethylamino) ethylamine showed good adsorption capacity and higher selectivity towards CO_2 in the presence of gases such as CH_4, N_2, O_2 and H_2 (Belmabkhout and Sayari 2009). Some of the common supports for grafting amine groups are MCM-41, pore expanded (PE) MCM-41, KIT-6, and SBA-15. The main difference between these supports are their geometry, pore volume and surface area. These are the main properties to consider when choosing the support as they play an important role in amine loadings. Pore size of the silica sorbents can be varied by modifying the synthesis process. A large pore volume can increase the distribution of amine groups in the pores because of lower mass transfer resistance (Kishor and Ghoshal 2017). The pore structure can affect the heat requirements for regeneration (Gatti *et al* 2017).

Amine groups, being basic, interact with the acidic CO_2 to form ammonium carbamate (equation 1) which is the reason for the selectivity towards CO_2 (Danckwerts 1979). Whereas methane does not have an available electron pair, so it is considered neutral and will not react with the amine group. Tertiary amines react better in the presence of water. They cannot form carbamates but in the presence of water they can form bicarbonate.

- $CO_2 + 2RNH_2 \leftrightarrow RNH_3^+ + RNHCOO^-$ (1)

CO_2 capture study with APTES immobilized on polyethyleneimine (PEI) showed an adsorption capacity up to 3.2 mmol/g sorbent at 60 °C adsorption temperature (Fauth *et al* 2012). Removal of CO_2 from CH_4 using SBA-15 as a porous support modified using primary amine APTES has been studied before to get an adsorption capacity of about 2 mmol/g sorbent at a regeneration pressure 10 kPa (Mafra *et al* 2017). Primary amines have a better balance between the working capacities and selectivity (Mafra *et al* 2017). In a PSA process, high selectivity also makes regeneration difficult. The effect of water has not been examined for APTES-SBA15. Table 2 provides a brief summary of literature on this subject.

CO_2/CH_4 separation using triethanolamine showed a CO_2 adsorption capacity of 1.75 mmol/g in the presence of CH4 and stable regeneration occurred up to 16 cycles (Liu *et al* 2017). TRI-PE-MCM-41 was examined to determine adsorption capacities of pure CO_2 and pure H_2S (Belmabkhout *et al* 2009a). CO_2 and H_2S isotherms were generated for a pressure up to 1.5 bar. At a pressure below 0.4 bar CO_2 adsorption was higher but at pressure above 0.4 bar H_2S adsorption was higher. At 1 bar, CO_2 and H_2S adsorption capacities were 2.4 and 3.4 mmol/g respectively. For 15% CO_2 using tetraethylenepentamine (TEPA), an adsorption capacity of 2.45 mmol/g was seen which increased to 3.01 mmol/g on addition of 2-amino-2-methyl-L-propanol (AMP) as a promoter. 15 cycles of adsorption showed stable adsorption capacities. Water enhances the adsorption capacities of the amine groups and tertiary amines cannot react with CO_2 in the absence of water (Liu *et al* 2017). For amine grafted adsorbents, the presence of water enhances the CO_2 adsorption because of the formation of bicarbonate (equation 2).

- $CO_2 + R_1\ R_2NH + H_2O \leftrightarrow\ R_1R_2NH_2^+HCO_3^-$ (2)

H_2S is a contaminant in LFG and usually needs to be removed prior to CO_2 removal process. Amine groups are basic in nature and interacts strongly with both CO_2 and H_2S as they are acid gases. So, they compete with CO_2, if present during the CO_2 removal process. Some of the common H_2S adsorbents like activated carbon and zeolites do not work well in the presence of water. In fact, it reduces the strength of the adsorbent and increases the regeneration heat required because of strongly bound CO_2.

Table 3. Summary of CO_2 adsorption using various amine grafted supports

Support	**Amine Used**	**Adsorption capacity (mmol/g)**	**Comments**	**Ref**
MCM-41	-	5.4	PSA process for pure CO_2 adsorption, Enhanced CO_2 selectivity at 25 bar	(Belmabkhout and Sayari 2009)
PE-MCM-41	TRI	1.6	Higher selectivity of CO_2 over N_2, CH_4, H_2 and O_2 Water vapor increased adsorption capacity	(Belmabkhout *et al* 2010a)
SBA15	APTES TMMAP 3-DEAPTES	0.8 1 <0.5	Even though TMMAP (2^o), 3-DEAPTES (3^o) have higher selectivity, they have low working capacities for application in cyclic processes like PSA. APTES is a better compromise between the high selectivity for CO_2 and a reasonable working capacity PSA used for studies	(Mafra *et al* 2017)

PE-MCM-41	TRI	2.4 3.4	Pure CO_2 adsorption Pure H_2S adsorption	(Belmabkhout *et al* 2009a)
SBA-15	triethanolamine	1.75	CO_2/CH_4 separations Stable adsorption for 16 cycles	(Liu *et al* 2017)
MCM – 41	MCM-41-TEPA60% MCM-41-AMP30% MCM-41-TEPA30%-AMP30%	2.45 1.79 3.01	15% CO_2 removal Addition of promoter increased CO_2 adsorption Presence of O_2, H_2O, etc. and their effects on CO_2 capture not studied.	(Wang *et al* 2015)

Regeneration of the adsorbent and its stability plays a key role for its usage over time. The adsorption of CO_2 on APTES loaded over mesoporous KIT-1 has been studied before and it was found that the adsorption capacity remained constant for up to 10 cycles (Kishor and Ghoshal 2015). The regeneration was done at 120 °C. TRI-amine, (3-trimethoxysilylpropyl) diethylenetriamine (TA) showed only a slight loss in CO_2 adsorption capacity after 24 adsorption-desorption cycle done at 60 °C and 120 °C respectively for a 15% CO_2 feed (Chang *et al* 2009). In the same study, it was shown that for TA modified silica, the adsorption capacity improved in the presence of water (78% RH). For a 40 adsorption-desorption cycles, APTES modified PE-MCM-41 showed a deactivation of 45% under dry conditions. The reason for deactivation could be the formation of urea groups, which can be restored by heating the adsorbent at temperatures up to 200 °C in humid conditions.

Based on the literature review, amine modified silica has high affinity to CO_2 and has a high potential to be used for CO_2 adsorption process from LFG for simultaneous removal of water and CO_2. Both PSA and TSA process can be used for the adsorption processes. The adsorption can be carried out at room temperature and at higher temperatures, above 80 °C desorption starts taking place. The easy reversibility of the reaction and its high adsorption capacity makes it very promising candidate for carbon dioxide capture. The objective of this work is to evaluate its effectiveness for purifying landfill gas contaminated with impurities. In particular, the effect of water and methane on adsorption capacity is of interest.

3. METHODS USED

3.1 Synthesis Methods

Chemicals required for the synthesis were purchased from Sigma-Aldrich unless mentioned otherwise and used as-received. The chemicals used include copolymer $(EO)_{20}(PO)_{70}$ $(EO)_{20}$ (P123), tetraethyl orthosilicate (TEOS >98%), HCl (37%, w/w), APTES (>99%), toluene (>99.5%), and acetone (>99.5%).

3.1.1 Synthesis of SBA-15

SBA-15 was used as the mesoporous silica support for the adsorbent. Due to its large pore volume and pore diameter, it is suitable for functionalization by large molecules. The SBA-15 was synthesized hydrothermally using the procedure reported (Cano *et al* 2011). In the synthesis of SBA-15, TEOS is the silica source and P123 copolymer acts as the structure directing agent. Figure 7 shows SBA-15 synthesis procedure.

For the SBA-15 preparation in this work, 6.0 g of copolymer P123 $(EO)_{20}(PO)_{70}$ $(EO)_{20}$ (Aldrich) was dissolved in 180 ml DI water. To this, 30 ml of HCl solution was added. After the solution was continuously stirred for 3 h at 40 °C on a hot plate, a volume of 13.5 ml of TEOS was added dropwise to the solution. The solution was kept stirring at 40 °C for 24 h. The mixture was kept to age at 110 °C for 8 h in a tightly sealed container. Finally, the solid was recovered by centrifuging and washing it multiple times with DI water. The SBA-15 was left overnight to dry at room temperature. Calcination was done at 500 °C with a ramp rate of 1 °C/min for 6 h.

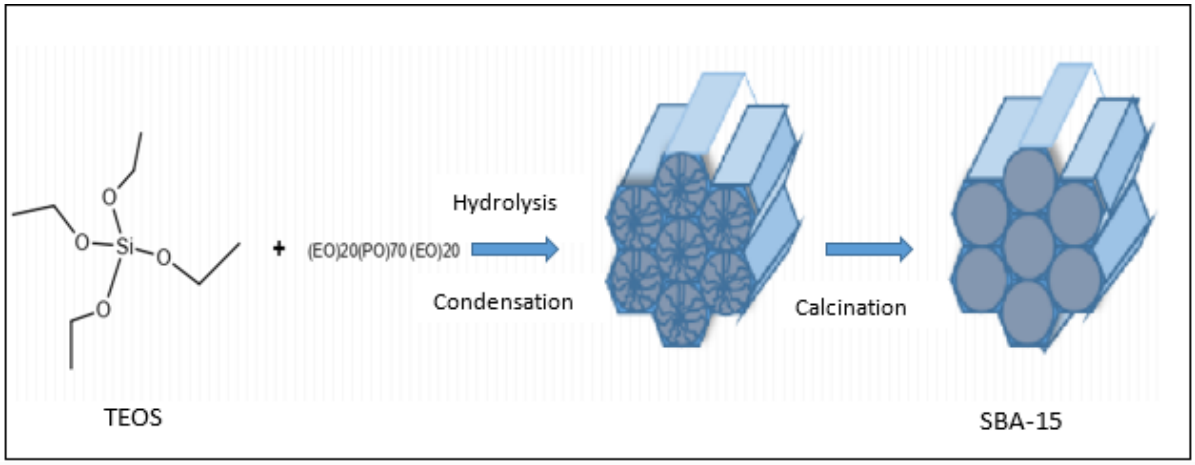

Figure 7. SBA-15 synthesis process. Figure adapted from V. Chaudhary (Chaudhary and Sharma 2017)

3.1.2 Synthesis of APTES Modified SBA-15

Synthesis of APTES modified silica was done by techniques reported in previous studies (Kumar *et al* 2013) with some modifications and scaling down. SBA-15 (1 g) was added to 20 ml of toluene in a round bottom flask. To this, a measured amount of APTES was added and the solution refluxed for 16 h at 120 °C with vigorous stirring. The solid recovered using vacuum filtration was washed with toluene, acetone and DI water in the same order. The obtained solid was dried overnight at 100 °C. Figure 8 shows SBA-15 functionalization procedure using APTES.

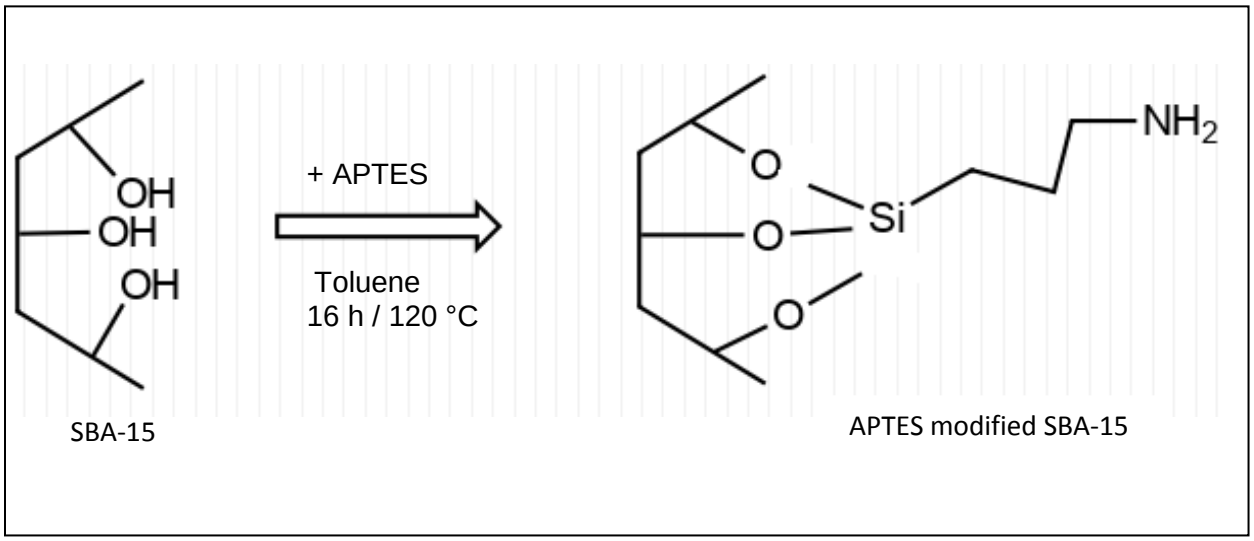

Figure 8. Surface functionalization of SBA-15. Figure adapted from Teng, W., et al. (Teng *et al* 2013)

3.2 Characterization Methods

All the pure gases used in the experiments were from Airgas with ultra-high purity >99.999% unless noted otherwise. CO_2 gas used was of Instrument grade with 99.99% purity. LFG used for the experiment was from Sarasota County's MSW Landfill with a composition of 56.7% CH_4 and 40.5% CO_2, with the remainder air (2.8%). The main contaminants were hydrogen sulfide (68 ppm) and siloxanes (4 ppm). More information provided in previous study (Zhao *et al* 2019).

X-ray diffraction (XRD), physisorption, Fourier-transform infrared spectroscopy (FTIR), and Temperature-Programmed Oxidation (TPO) were used to characterize the samples. XRD analysis was done using a Bruker AXS instrument. Cu Kα radiation (0.154 nm) was used to get the XRD diffraction patterns. A Bragg angle (2θ°) in the range of 20-90^0, with a step size of 0.02 was used with a dwell time of 1.5 sec for each step.

N_2 physisorption was done to get the adsorption-desorption isotherms using a Quantachrome Autosorb – iQ at 77K. The samples were outgassed at 200 °C before adsorption. Brunauer – Emmett-Teller (BET) method was used to calculate the surface area inside the range of relative pressure from 0.05 to 0.3 and Barrett-Joyner-Halenda (BJH) method was used to find the pore size distribution of the samples by determining the volume of N_2 adsorbed at a set interval of relative pressures (P/P_0).

To examine the different bonds in the samples, FTIR was done in a Nicolet IS50 instrument from Thermo-Scientific in attenuated total reflection (ATR) mode. The spectra scan comprised of 50 scans with a data spacing of 0.482 cm^{-1}.

TPO was carried out to study the actual loading of APTES on SBA-15. Approximately, 80 mg of sample was taken for each experiment. It was carried out in a U-tube reactor inside a Thermoscientific Thermolyne tube furnace. The samples were pretreated at 100 °C for 2 h before starting the experiment in 30 sccm of He. MKS Cirrus mass spectrometer (MS) connected in line with the reactor was used to monitor the signals. Upon stabilization of signal, 5% by vol O_2/He was flowed until the signal became stable. Finally, the samples were heated to 800 °C at a rate of 10 °C/min and held for 1 hour. Output signals were monitored at 10 sec intervals. The area under the curve is used to calculate the total C content in the sample.

To validate the TPO data, calcination experiments were also carried out for all the samples to study the actual loading of the sample. For this, sample masses of 1 g with different APTES loadings were pretreated at 150 °C for 2 h to remove any moisture. It was weighed again before heating it to 800 °C for 1 h. The final sample was weighed again after cooling to room temperature.

3.3 Adsorption Testing Methods

For all the experiments, around 80 mg of sample was taken in U-tube quartz reactor with approximately an outer diameter of 4 mm and length 120 mm. In the reactor, the sample was positioned between glass wools (Figure 9). The reactor was placed inside a furnace with a 10 °C/min ramp rate. All flow to the reactor was controlled using Alicat mass flow controllers. A mass spectrometer (MS) connected in line with the reactor was used to monitor the signals and get data every 10 sec. Before experiments, samples were heated to 200 °C for 2 h to remove any adsorbed gases and moisture by passing helium gas. It was then cooled back to room temperature which took approximately 4 h. Adsorption was carried out at room temperature and desorption at 100 °C. For the adsorption test, gases were flown for 30 min to ensure complete saturation of the bed.

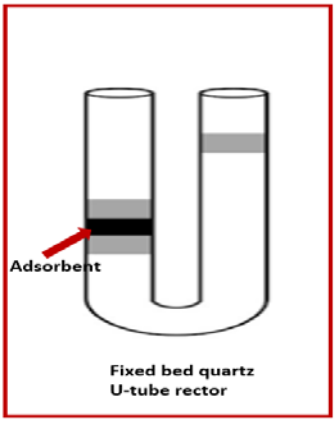

Figure 9. U-tube reactor used for the experiment

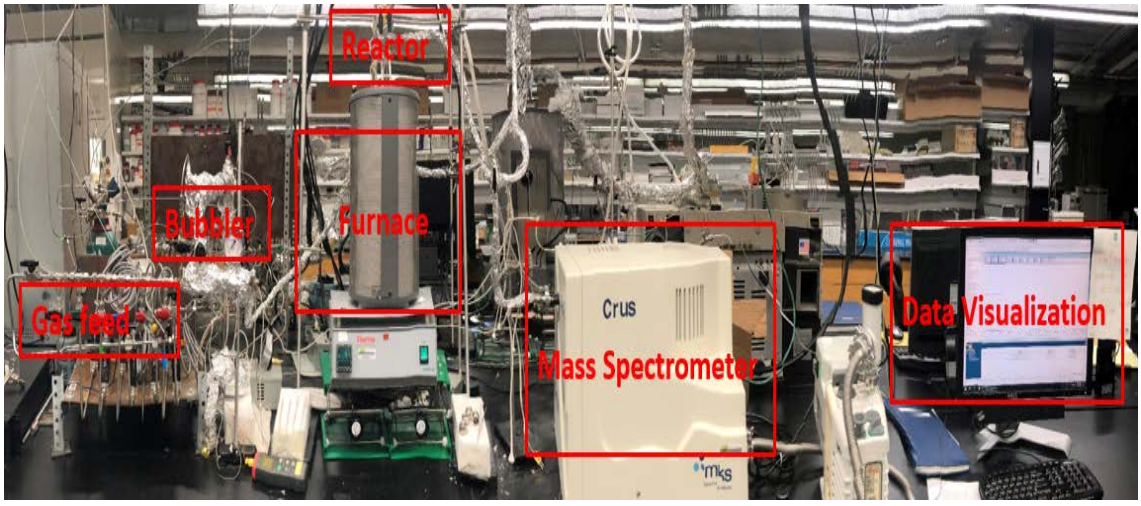

Figure 10. Experimental set-up for gas adsorption studies

3.3.1 Pure CO_2 Adsorption

To study the CO_2 adsorption capacity of the sample, 50% CO_2/He flowed to the sample for 30 min followed by the desorption test at 100 °C. A total flow rate to 30 sccm was used. Signals were allowed to stabilize before both steps. The experimental set up for these studies is shown is Figure 10.

CO_2 adsorption study was done to get the adsorption-desorption isotherms using a Quantachrome Autosorb – iQ at room temperature. Approximately 55 mg of sample was outgassed at 200 °C

before adsorption. The adsorption temperature was maintained at room temperature using a dewar filled with water.

3.3.2 Adsorption of CO_2/CH_4 Mixture in Dry Conditions

To study the affinity of the sample towards CO_2 in a gas mixture with concentrations similar to LFG, 50% He and dry CO_2/CH_4 feed in the ratio 1:1 flowed to the samples for 30 min followed by the desorption test. A total flow rate to 40 sccm was used. Adsorbent regeneration was studied. For this, the adsorbent was regenerated at 100 °C and 5 cycles of adsorption-desorption were conducted.

3.3.3 Adsorption of CO_2/CH_4 Mixture in Humid Conditions

Experiments were done to study the effect of moisture on CO_2 adsorption capacity in a gas mixture with concentrations similar to LFG. For that, 10 sccm He and 30 sccm dry CO_2/CH_4 feed in the ratio 1:1 was used. He was flowed through a bubbler system set at a calculated temperature such that the total flow rate of He is always 10 sccm (Appendix D). A total flow rate to 40 sccm ($He+CH_4+CO_2$) was used. The gas mixture flowed through the sample for 30 min followed by the desorption test. Regeneration study done for 5 cycles. The bubbler set-up used for the experiment is shown in Figure 11.

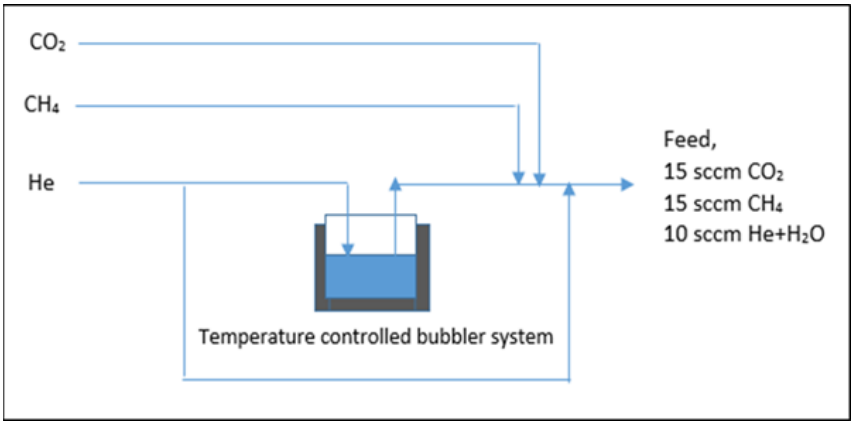

Figure 11. Bubbler set-up for CO_2 adsorption in humid conditions.

3.3.4 LFG Adsorption Studies

LFG adsorption on the adsorbent was done in a similar procedure and apparatus. A flow of 30 sccm of LFG in a total flow rate of 40 sccm (balance He) was sent through the sample for 30 min.

Desorption was carried out at 100 °C after CO_2 signal stabilization. Regeneration study was done for 5 cycles.

4. RESULTS AND DISCUSSIONS

4.1 Synthesis Results

APTES functionalized SBA-15 with different loadings of APTES were synthesized to determine the CO_2 adsorption capacity of the adsorbents. The adsorbent synthesis was done via grafting method using SBA-15 as the support and immobilizing APTES on it. To achieve different loadings of the amine on silica, different amounts of APTES (0.3, 1.0, 1.4, and 2.5 mL) was added to 1 g of SBA-15 (using toluene as solvent) during the synthesis process. It is to be noted that not all APTES added was attached on to the SBA-15, as some of it was lost during the washing step with toluene in the synthesis process. To have a better assessment of the loading of APTES to the support, 1 g of the sample was calcined at 800 °C and the weight loss was measured. At this high temperature, all organic material will be removed via combustion, and the weight loss can be accounted for the amount of APTES in the sample. Appendix B shows the weight percent calculations of the calcination experiment. Also, to confirm the results, temperature programmed oxidation (TPO) was carried to find the weight percent of APTES on silica. The summary is given in Table 4. The nomenclature is based on the second to final column, though the TPO results were very similar.

Table 4. Comparison of wt % obtained from calcination with wt % obtained from TPO. 1 g of adsorbent was the initial weight.

Sample	Amount of APTES added (ml)	Weight of APTES added (g)	Weight % from calcination experiment	Weight % from TPO
12wt%APTES	0.3	0.28	12	14
20wt%APTES	1.0	0.95	20	18
26wt%APTES	1.4	1.32	26	28
25wt%APTES	2.5	2.36	25	25

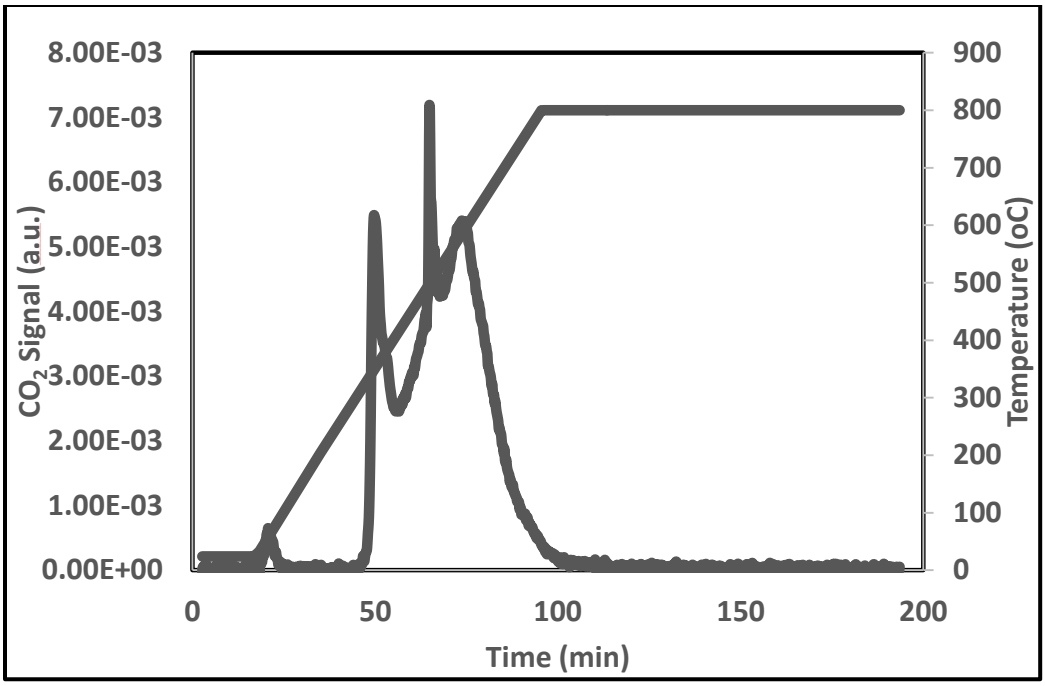

Figure 12. CO_2 signal from TPO graph for 12wt%APTES

Figure 12 shows the CO_2 signal from TPO experiment of 12wt%APTES. The first peak corresponds to CO_2 desorption due to CO_2 adsorbed from the air. The peak after 300 °C corresponds to the CO_2 from the organic compound which was quantified to find the weight percent of APTES in the sample using carbon balance (see APPENDIX E).

4.2 Characterization Results

The samples prepared were characterized using XRD. The XRD results for SBA-15 without any loading and 12wt%APTES are presented in Figure 13. The line positions for the sample did not change much, but the intensity decreased for APTES-SBA15. This is due to pore filling of the SBA-15.

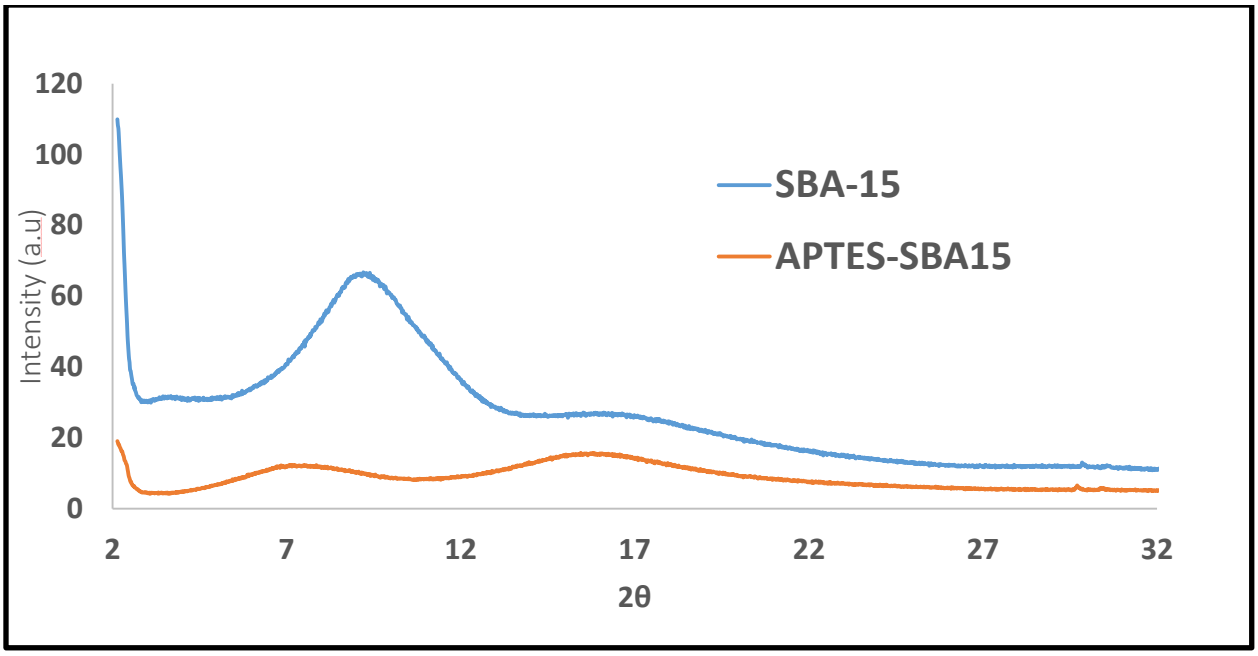

Figure 13. XRD profiles of SBA-15 and 12wt%APTES-SBA-15

Surface areas of the samples were found using the BET method and pore distribution of the samples were calculated using the BJH method. The results are presented in Table 5. The surface areas of the silica decreased once the APTES is added. 26wt%APTES showed the least surface area, as it has the highest loading. The pore volume of the SBA-15 is significantly reduced after functionalization which confirms the functionalization of the amine on SBA-15. 26wt%APTES after reaction with LFG showed a significant decrease in pore volume. Figure 14 shows the N_2 adsorption and desorption isotherms for SBA-15, 12wt%APTES, 20wt%APTES, 26wt%APTES and 26wt%APTES post adsorption with LFG after 5 cycles.

Table 5. Pore size distribution of adsorbents before adsorption studies and 26wt%APTES post CO_2 adsorption/desorption with LFG after 5 regeneration cycles

Sample	Surface area (m^2/g)	Pore Volume (cc/g)	Avg. Pore Diameter (nm)
SBA-15	672	0.81	7.8
12wt%APTES	354	0.51	6.1
20wt%APTES	349	0.50	5.6
26wt%APTES	168	0.26	5.6
26wt%APTESpost	178	0.29	5.7

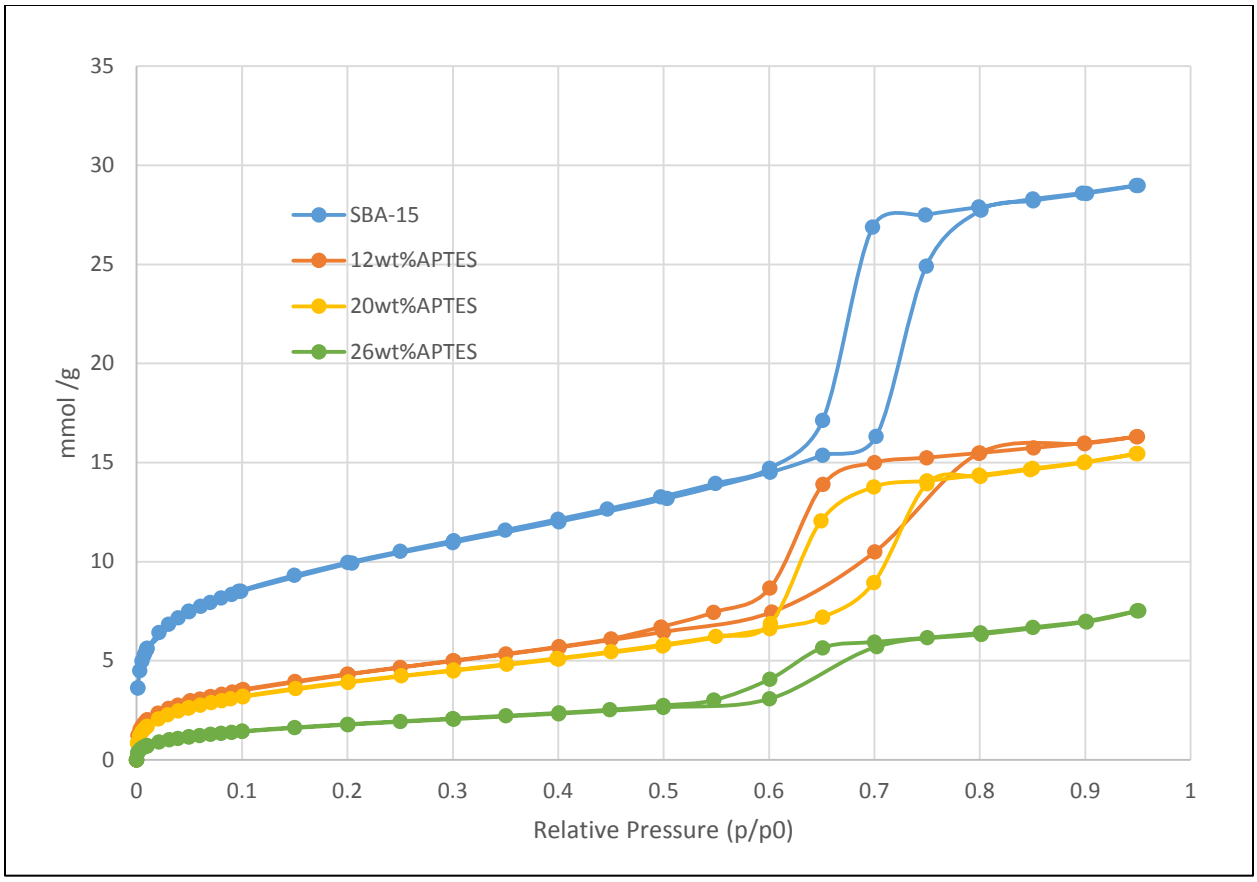

Figure 14. N_2 adsorption-desorption isotherms for SBA-15 and various loadings of APTES-SBA15

SBA-15 without any loading adsorbs the highest amount of N_2. After functionalization, the adsorption decreases with increased loading of APTES. This is because, the pores of SBA-15 are blocked by the large amine groups present. So, less surface area is available for N_2 adsorption. All the samples exhibit a similar hysteresis loop which confirms that the SBA-15 characteristics were retained in the final sample. The initial adsorption is due to the monolayer adsorption of N_2 followed by multilayer adsorption. At higher pressures, there is a limiting uptake of N_2 which can be associated with possible condensation of gas in the capillary pores. The slimming of the hysteresis is because of the decrease in pore volume and surface area. Pore size distributions of the samples are shown in Figure 15.

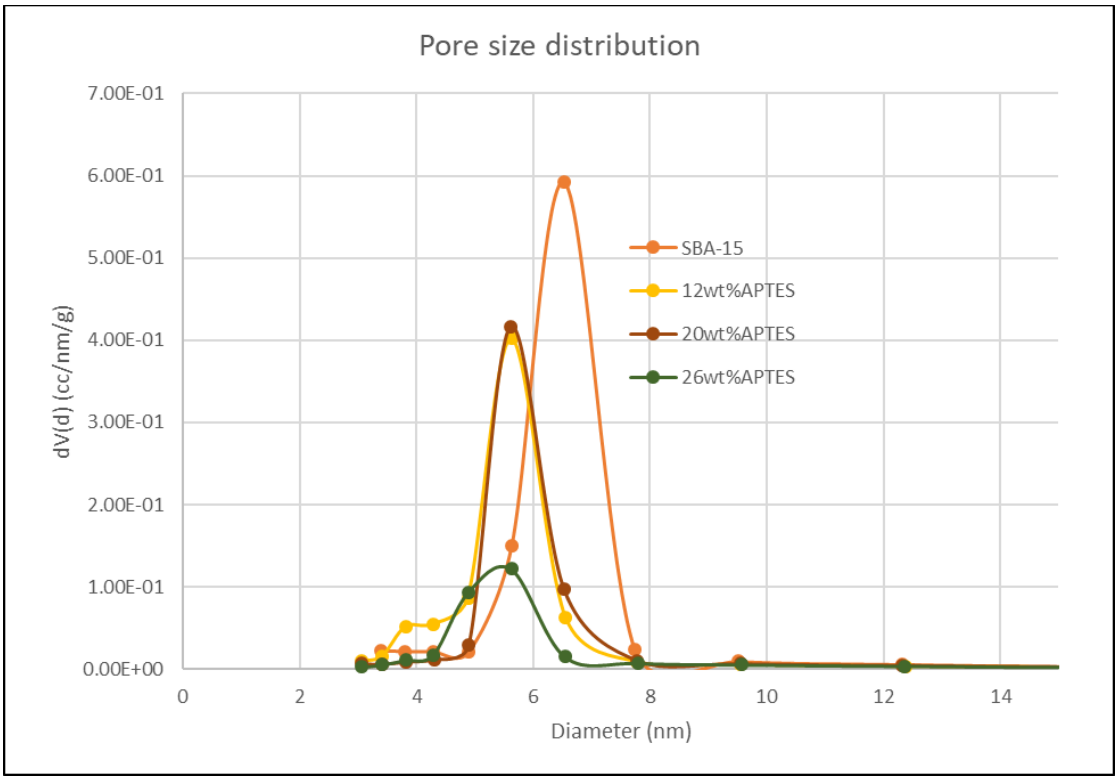

Figure 15. BJH pore size distribution of SBA-15 and various loadings of APTES-SBA15

FTIR spectroscopy characterization was used to detect the chemical functionality of the adsorbents. Figure 16 shows the FTIR results for SBA-15 and SBA-15 with different APTES loadings. The broad peak at 3440 cm^{-1} represent Si-O-H group in SBA-15 and the peak at 1080 cm^{-1} represent Si-O-Si anti symmetrical stretching vibrations. The C-N stretching and C-N-H bending vibrations are observed through bands 1570cm^{-1} and the bands around 1320 cm^{-1} indicates H-C-H rocking and twisting. C=O and C-H stretching are detected by 1650 and 2970 cm^{-1} respectively (Kumar *et al* 2013).

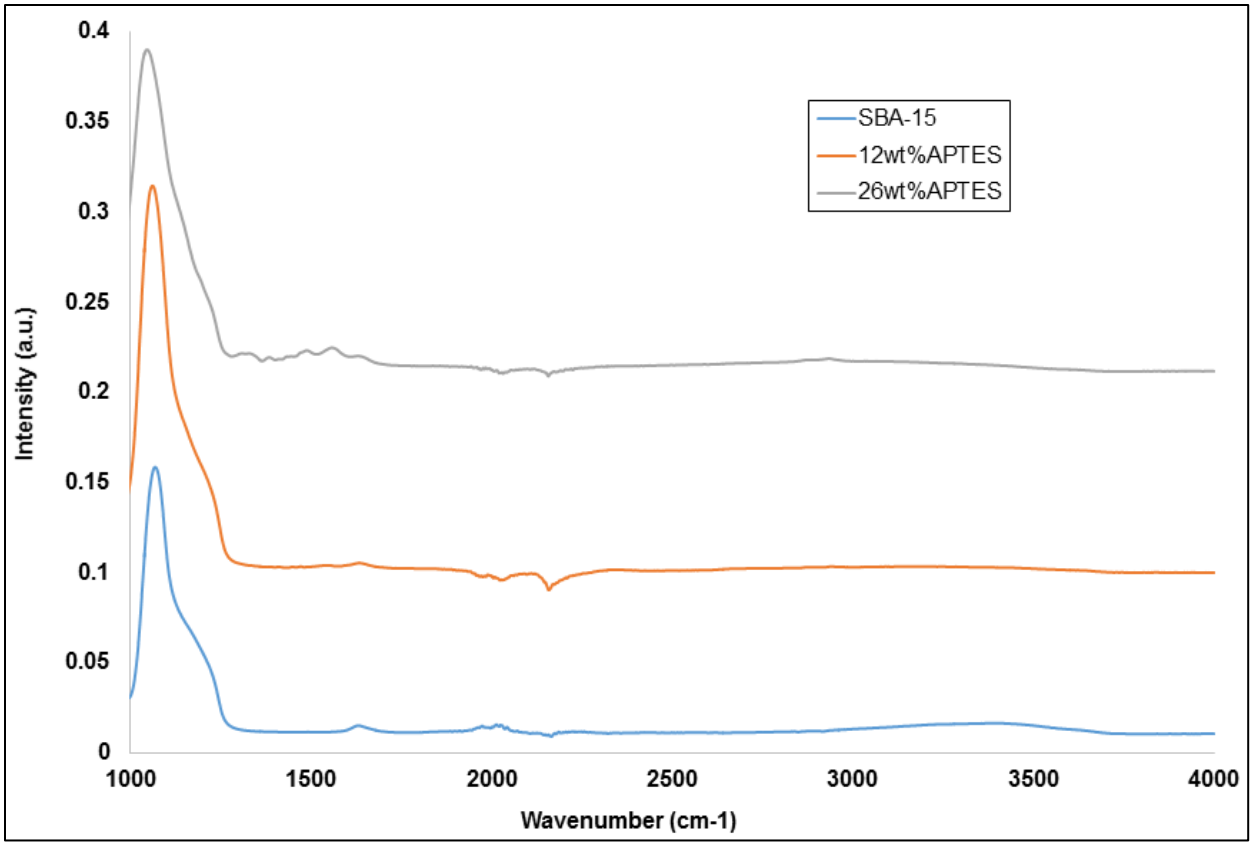

Figure 16: FTIR spectra of SBA-15 and APTES-SBA15

4.3 Adsorption Study Results

CO_2 adsorption study was carried out at room temperature and 1 atm pressure on SBA-15, 12wt% APTES/SBA-15, 20wt% APTES/SBA-15, and 26wt% APTES/SBA-15. Figure 17 shows how the adsorption capacity of the APTES–SBA15 varies as the amine loading increases. SBA-15 without any loading has the lowest adsorption capacity with adsorbing only 0.016 mmol/g. As the APTES content in the sample increases from 12 to 26 wt%, the adsorption capacity also increases from 0.069 to 0.85 mmol/g. This value is comparable to the 1 mmol/g CO_2 adsorption capacity obtained before (Mafra *et al* 2017) for APTES/SBA-15 adsorbent. More details on the adsorption capacity calculations and repeatability of the experiments are given in Appendix C and G, respectively.

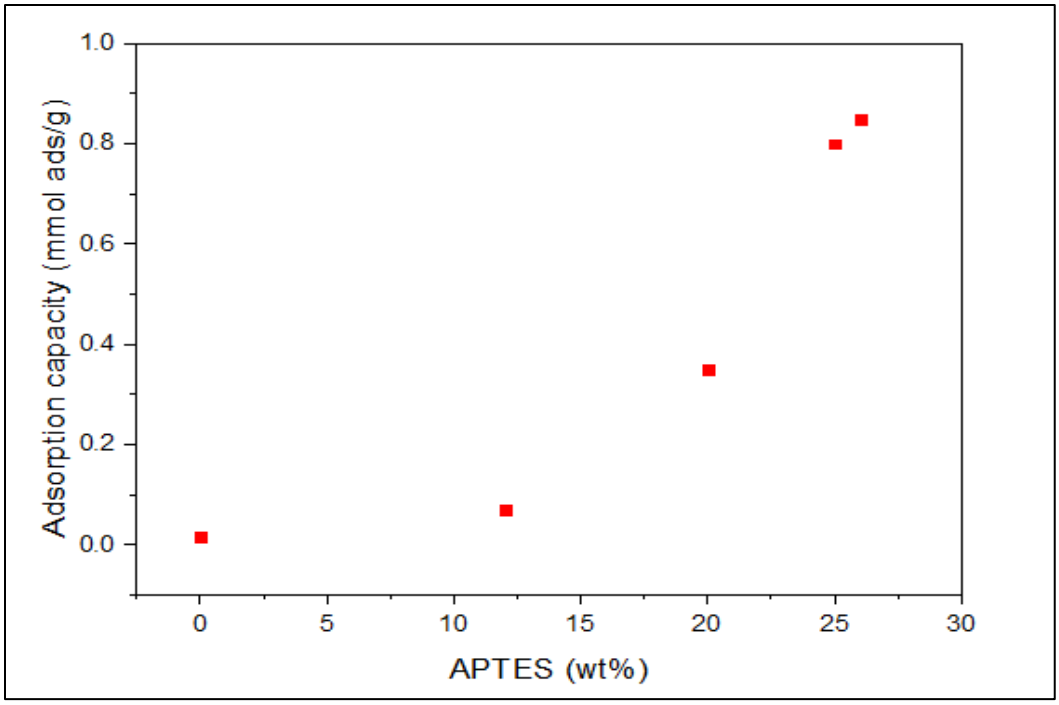

Figure 17. CO_2 adsorption capacities of SBA-15 and APTES-SBA15

CO_2 adsorption-desorption isotherms were generated for the SBA-15 and APTES modified SBA-15 samples as shown in Figure 18. SBA-15, at high relative pressure, shows an adsorption capacity of 1.13 mmol/g. SBA-15 has high surface area, so at higher relative pressures pore filling only because of physical adsorption takes place. Functionalization of SBA-15 results in steeper adsorption hysteresis at relative pressures lower than 0.1. This is due to the chemical adsorption of CO_2 on the amine group. The highest adsorption capacity of 1.41 mmol/g is achieved by 26wt%APTES at higher relative pressures.

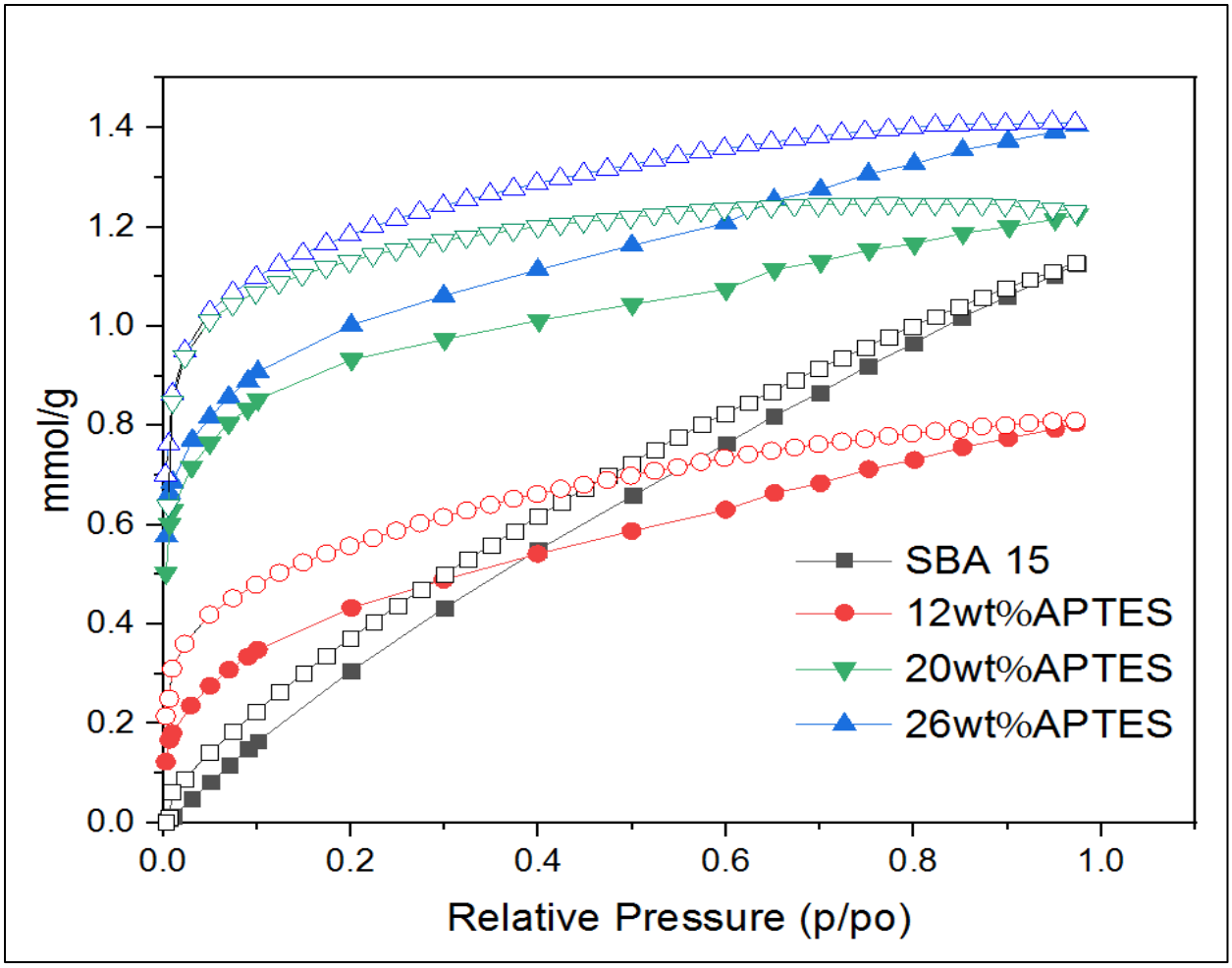

Figure 18. CO_2 adsorption-desorption isotherms of SBA-15 and various loadings of APTES-SBA15. Solid and hollow symbols indicate adsorption and desorption branches, respectively.

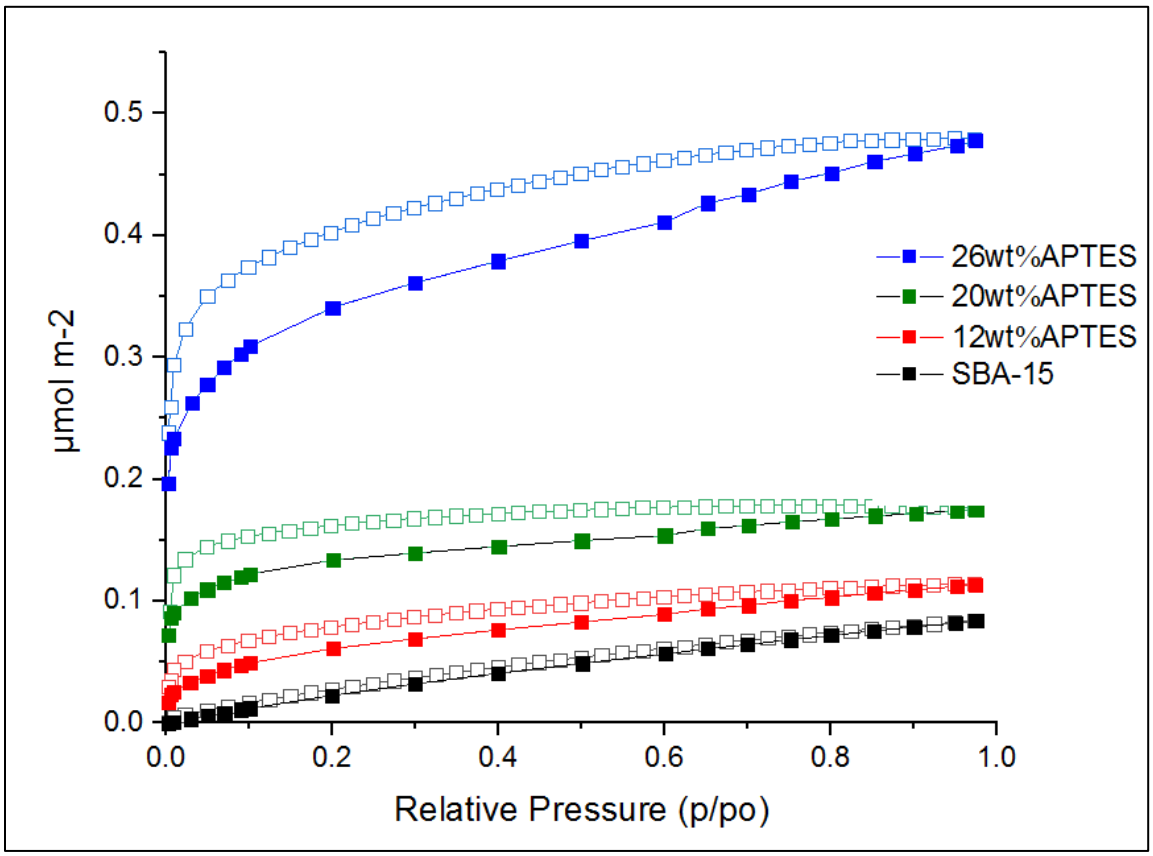

Figure 19. CO_2 adsorption-desorption per surface area of the adsorbent. Solid and hollow symbols indicate adsorption and desorption branches, respectively.

Adsorption capacity increased as the amine loading increase however at higher relative pressures SBA-15 showed better adsorption capacity than 12wt%APTES. Because of the low loading in 12wt%APTES, at lower relative pressures all the available amine groups could have reacted with CO_2. At higher relative pressures, there is no more amine groups to react with CO_2 and the adsorption is only due to pore filling. SBA-15 with higher surface area and pore volume will therefore have better adsorption. Figure 19 explains this better. This is also the reason why samples with higher loading has only a small increase in adsorption capacity at higher relative pressures.

To study the adsorbent performance in CO_2/CH_4 mixture, adsorption/desorption was carried out in a total flow rate of 40 sccm with 30 sccm CO_2/CH_4 in 1:1 ratio. The experiment was done using the 26wt%APTES, as it gave the highest adsorption capacity. The adsorption capacity of the sample in the mixture was 0.83 mmol/g compared to 0.85 mmol/g in pure CO_2. Hence, the adsorbent has high affinity to CO_2. Figure 20 shows the breakthrough curve of CH_4/CO_2 adsorption on 26wt%APTES-SBA15,

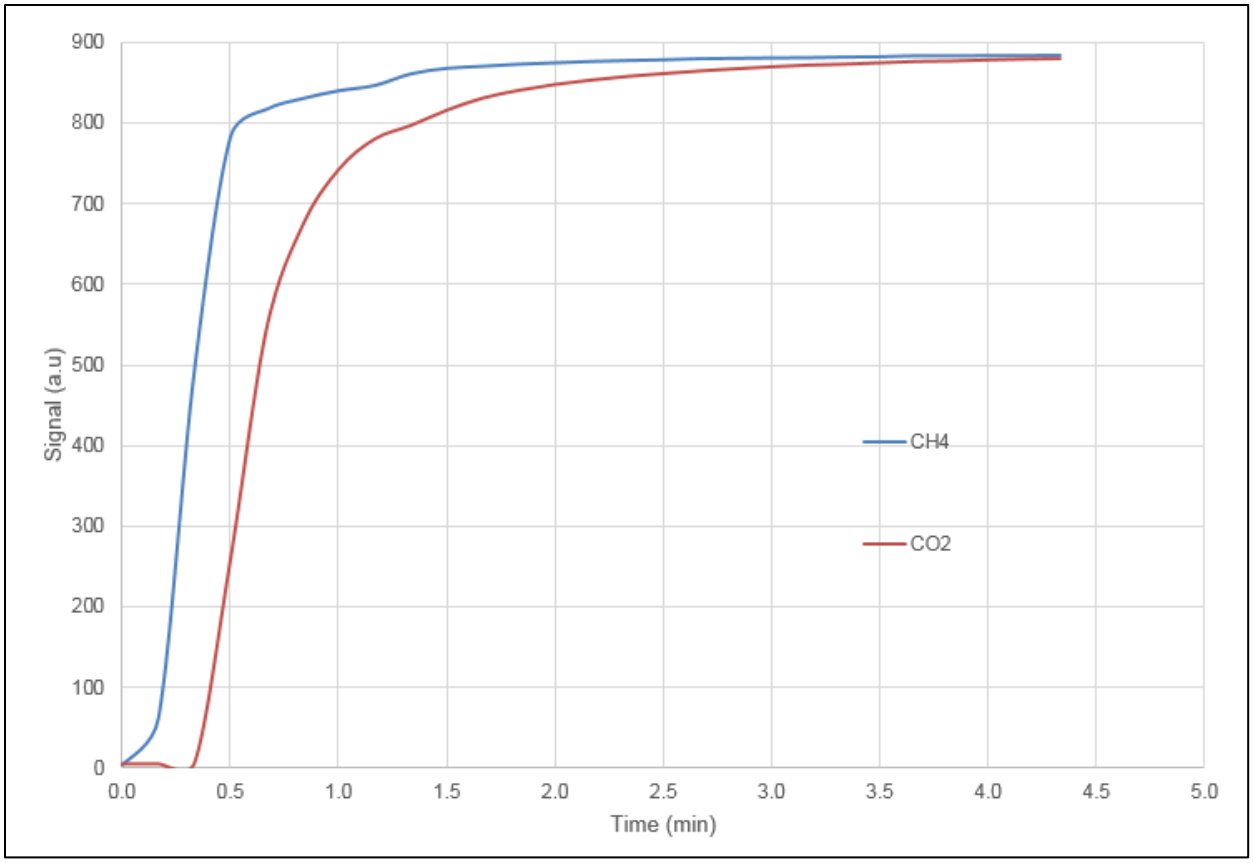

Figure 20. CH_4/CO_2 breakthrough curve on 26wt%APTES-SBA15

LFG contains moisture so it is important to study the effect of water on the adsorbent. For that, different amount of water vapor was flown through the 26wt%APTES adsorbent bed along with CO_2/CH_4. The results are presented in Table 6.

Table 6. CO_2 adsorption in the presence of water in a total feed flow rate of 40 sccm (10 sccm He+H_2O, 15 sccm CH_4 and 15 sccm CO_2)

Water vapor flow rate (sccm)	CO_2 adsorption (mmol/g)	H_2O adsorption (mmol/g)
Dry	0.79	0.009
0.20	0.71	0.24
0.67	0.72	0.30
1.7	0.72	0.41

From Table 6, as the water content in the feed increases, the water adsorption by the sample increases. With dry CO_2, there is a small amount of water adsorbed, which is from the CO_2 cylinder. Increasing the water content in the feed leads to a slight decrease in the CO_2 adsorption capacity, which decreases from 0.78 to 0.72 mmol/g. Water might block a small portion of the adsorption sites or slow the mass transfer into the pores. Either could be reasons for decreased adsorption capacity. On further increase in water content in feed from 0.20 to 1.7 sccm, adsorption of water increases; however, CO_2 adsorption remains constant at 0.72 mmol/g. SBA-15 has affinity towards water, which is the reason there is water adsorption in the process. This only minimally impacts the CO_2 adsorption.

It is very important that the adsorbent should be able to be reused many times. So, it is important to study its regeneration properties to see if the adsorbent retains the adsorption capacity after several cycles of operation. Regeneration of the sample was carried out for 5 cycles in a total feed flow of 40 sccm with 1.7 sccm H_2O and 1:1 CO_2/CH_4. Figure 21 shows the adsorption capacities of CO_2 and H_2O as a function of cycle number. CO_2 adsorption remains constant at 0.72 mmol/g for the 5 cycles. Water adsorption varied between 0.2 and 0.40 mmol/g.

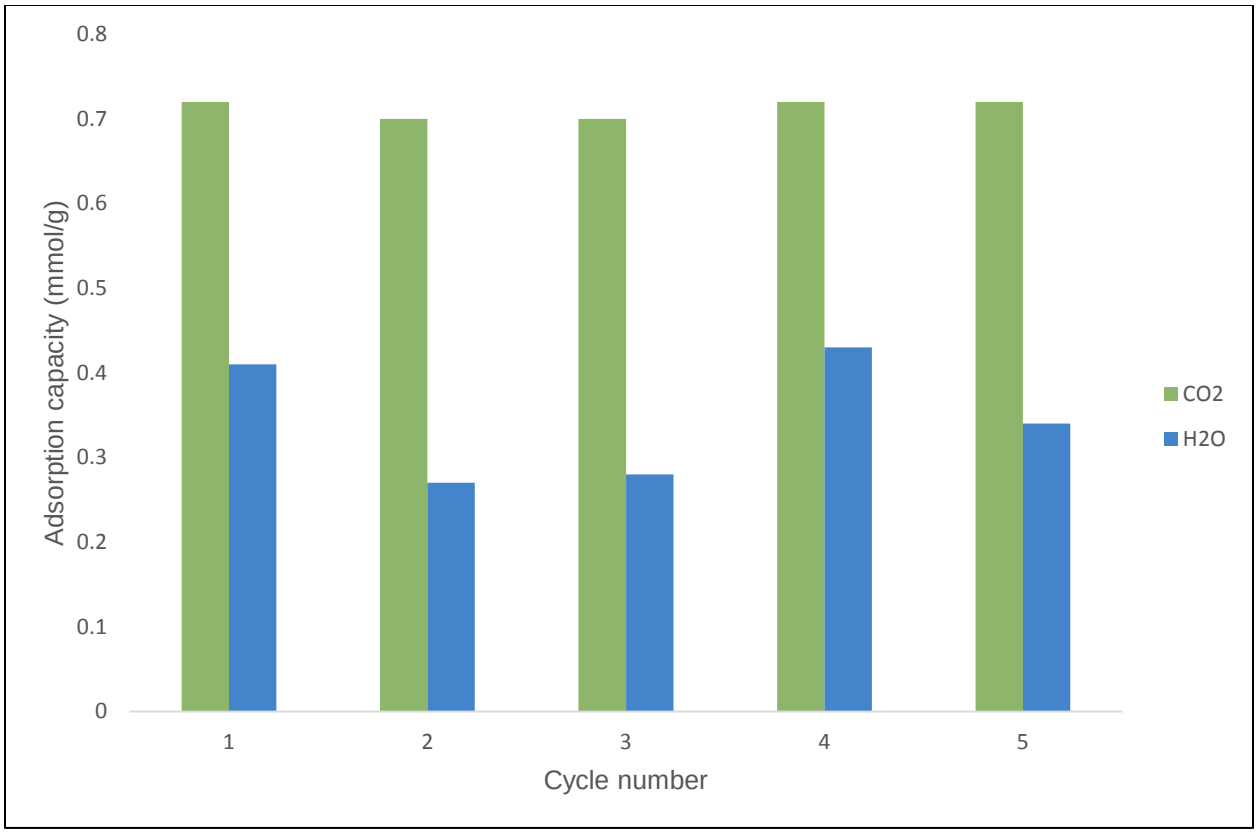

Figure 21. Cyclic regeneration of 26wt%APTES-SBA15. Adsorption of model biogas at T = 26 °C and desorption in He at T = 100 °C

Landfill gas contains other impurities like H_2, H_2S, N_2, siloxanes along with CO_2 and water. So, to see the adsorbents capability of removing CO_2 in the presence these impurities real LFG was used. The composition of the LFG used for the experiment shown in Table 5 was done in a previous study (Zhao *et al* 2019).

Table 7. LFG composition used for the experiment

Compound	**Mole percent (%)[a]**
CH_4	56.7
CO_2	40.5
N_2	2.4
O_2	0.4
H_2O	4-7 (vol%)
H_2S	68 (ppm)
CO	6 (ppm)
Siloxanes	4 (ppm)
Halides	3 (ppm)

[a] – Unless stated otherwise

It consisted of 56% CH_4, 40% CO_2, The CO_2 adsorption capacity of the adsorbent decreased to 0.55 mmol/g in the first cycle itself, when LFG was used. This can be because of the impurities in

the LFG which compete with the adsorption sites. H_2S like CO_2 are acid gases and amine groups have basic sites which results in the adsorption of these gases.

Table 8. Adsorption studies of 26wt%APTES-SBA15 for cycle 1 with pure CH_4/CO_2 and LFG as feed (adsorption of LFG at T = 26 °C and desorption in He at T = 100 °C)

Feed	CO_2 adsorption (mmol/g)	H_2O adsorption (mmol/g)
Pure CO_2	0.85	N/A
LFG	0.55	0.21

Again, to see the adsorbent stability and to learn if these impurities poison the adsorbent bed 5 regeneration cycles were carried out. The results are presented in Figure 22 CO_2 adsorption remained stable for the 5 adsorption cycles. The water adsorption also remained stable at approximately 0.2 mmol/g.

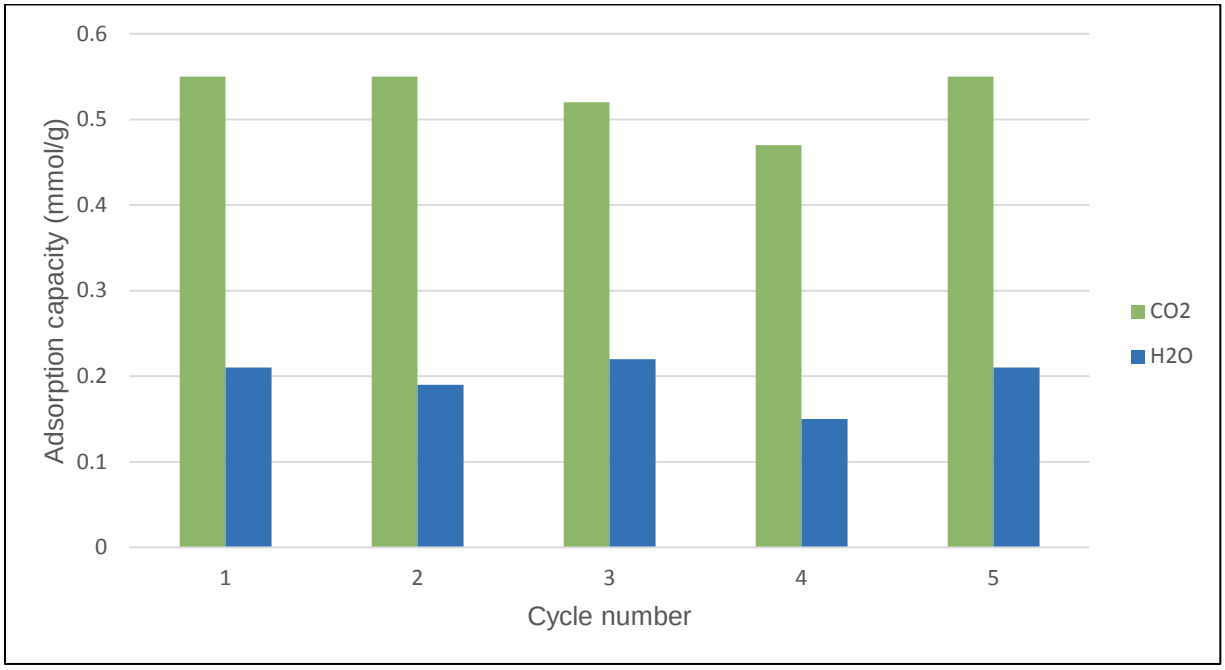

Figure 22. Cyclic regeneration of APTES-SBA15 with LFG as feed. Adsorption of LFG at T = 26 °C and desorption in He at T = 100 °C

Figure 23 shows a comparison of CO_2 adsorption in a mixture of dry/humid (25% RH, APPENDIX F) CO_2/CH_4 as feed and LFG feed. The adsorption capacity decreases by almost 30 percent when LFG is used as feed, but through the cycles adsorption remains constant.

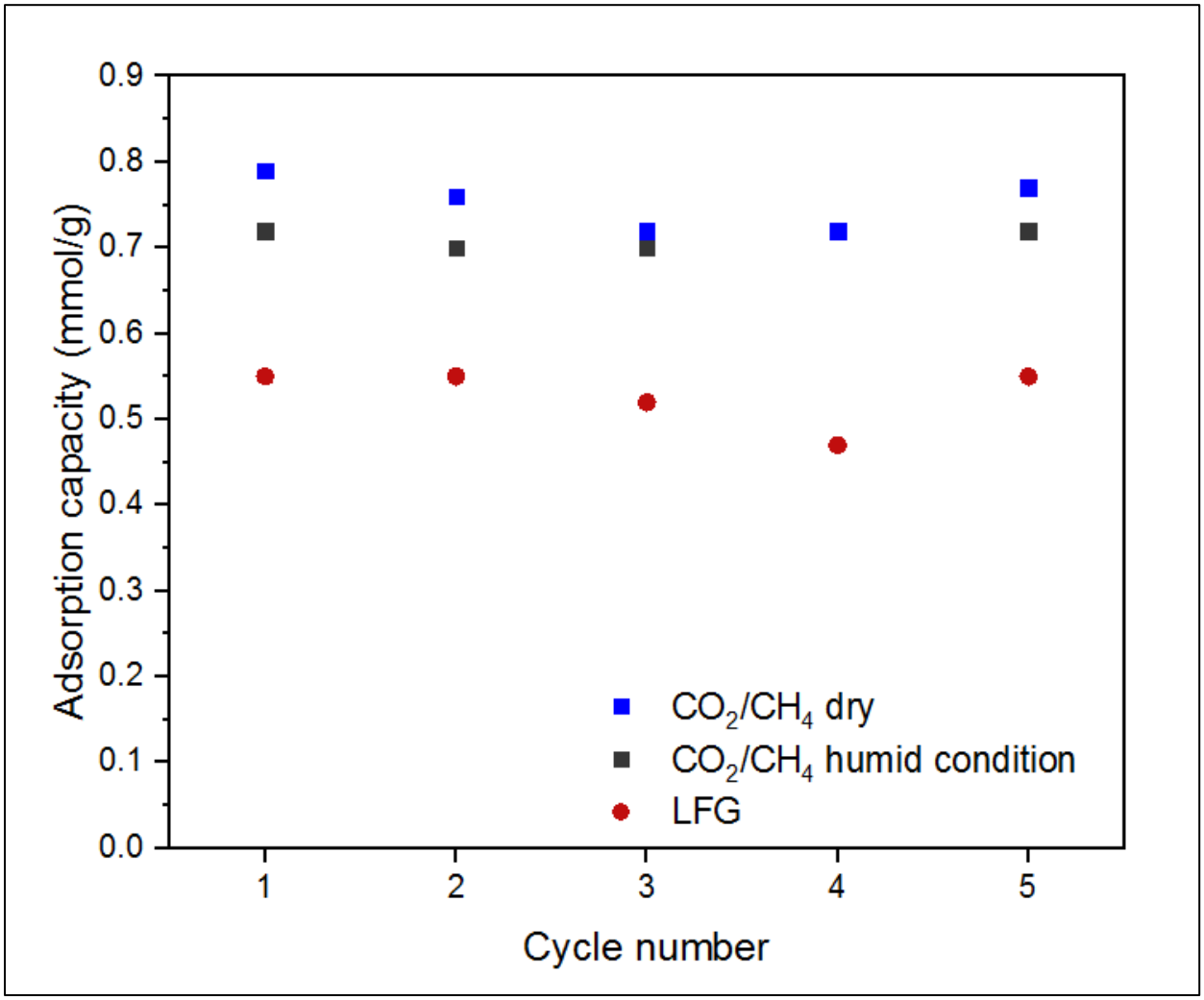

Figure 23. Comparison of CO_2 adsorption capacities with LFG and CO_2/CH_4 in dry and humid (25% RH) conditions as feed. Adsorption at T = 26 °C and desorption in He at T = 100 °C)

5. TECHNO-ECONOMIC ANALYSIS OF BIOGAS UPGRADING UNITS USING SUPPORTED AMINE SORBENTS (SAS)

5.1 Design and Modelling Approach of SAS CO_2 Units

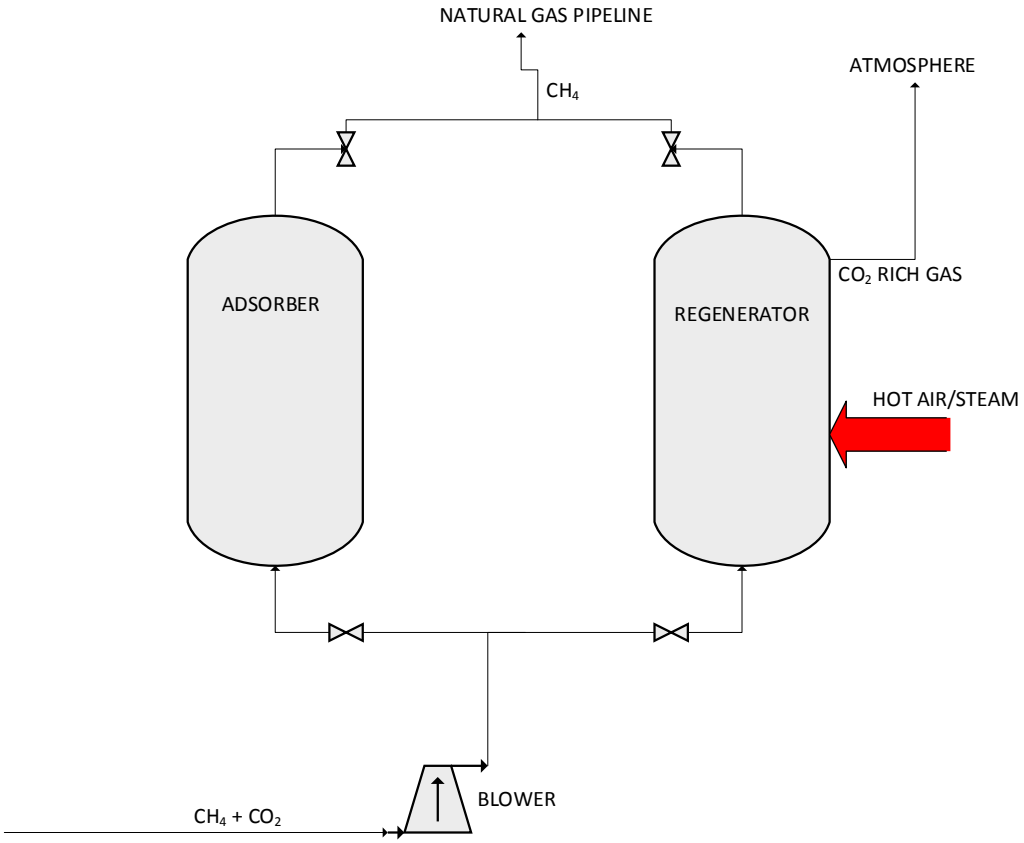

Figure 24. Schematic process model for a SAS unit for CO_2 removal from biogas. Either after sulfur removal or without sulfur removal

A fixed-bed adsorption system with a temperature swing for regeneration is considered. The reason for the selection of the fixed bed adsorption system is because of the higher level of operational simplicity and the expected lower investment costs. The fixed-bed adsorption system consists of a two-bed system, where one bed is in adsorption mode and the other is being regenerated. Once the adsorption bed is fully loaded with CO_2, a valve system switches the operating modes of the two beds. The adsorption step starts with the bed filled with sorbents that are regenerated until CO_2 lean conditions so that the CO_2 from the feed gas will be adsorbed until the gas phase CO_2 partial pressure is in equilibrium with the sorbent loading under lean conditions.

Equipment required for SAS units:

1. Process Vessel
2. Compressor/blower
3. Pipes and Valves

5.1.1 Typical SAS Units Design Conditions

The following basis and assumption were used to simulate the Supported Amine Sorbent (SAS) unit process performance:

- The process design conditions used are shown in Table 9. The feed composition is the average of a typical biogas composition (55%-65% CH_4, 35%-45% CO_2) after the removal of impurities. The feed pressure and temperature of a typical biogas plant are atmospheric pressure and room temperature respectively (Sutanto *et al* 2017a).
- The purity of the product is based on the national natural gas grid guideline (Mokhatab *et al* 2018). Methane losses at biogas upgrading plants are typically about 1.5% of upgraded biogas (Börjesson *et al* 2006).
- The height to diameter ratio of the adsorbing column is assumed to be 10 in order to reduce pressure drop across the column and increase the contact area between the feed gas and the sorbent.
- The sorbent was regenerated at 100 ℃(Gopalakrishnan 2019). The sorbent's longevity is assumed as six-month (2000 regeneration cycles).

Table 9. SAS design conditions

Feed composition	60% CH_4, 40% CO_2
Maximum feed flowrate, SCFM	2500 (Walas 1988)
CH_4 purity in product	98%
CH_4 loss	1.5%
Feed Pressure, bar	1
Feed Temperature, ℃	25
Regeneration Temperature, ℃	100
Source of heat for regeneration	Steam

Bed void volume	45% (Walas 1988)
Number of adsorbers	2
Adsorption time, hours	2
Process Vessel (Height to Diameter ratio)	10
Adsorbent density, kg/m^3	200.5
Adsorbate density, kg/m^3	1.977 (Wikipedia 2013)
Adsorbent heat capacity, J/kg.K	920 (AZoM 2019)
Adsorption capacity, $mmol_{CO2}/g_{ads}$	0.85 (Gopalakrishnan 2019)
Regeneration capacity, cycles	2000

$$Mass\ of\ adsorbent = \frac{Mass\ of\ adsorbate\ (Kg_{CO_2})}{Adsorption\ Capacity\ (\frac{Kg_{CO_2}}{Kg_{ads}})}$$

$$Mass\ of\ adsorbate = m_{CO_2} = Volumetric\ flowrate * Adsorbate\ density * Ratio\ of\ components * Adsorption\ time$$

$$Volume\ of\ adsorbent\ required = \frac{Mass\ of\ adsorbent\ required\ (Kg)}{Adsorbent\ density\ (kg/m^3)}$$

Volume of process vessel required = (1 + bed void volume) * Volume of adsorbent required

5.1.2 Economic Model

5.1.2.1 Estimation of Capital Cost/Fixed Capital Investment (FCI)

The fixed capital investment is the summation of the costs of major plant equipment and installation cost. The major equipment required as shown in Figure 24, includes two process vessels (adsorbers) and a compressor or blower to overcome pressure drop in the adsorbing column. The cost estimation of the vertical process vessel and compressor is based on volume capacity and fluid power, respectively, as in published correlations (Eqn 3 and Eqn 4) (Turton *et al* 2008). The total capital cost calculated is distributed over ten years and annualized in the operating cost of the plant.

Table 10. Equipment cost data used with Eqn. 3

Equipment type	Equipment Description	K_1	K_2	K_3	Capacity, A, units	
Process Vessel	Vertical	3.4974	0.4485	0.1074	Volume, m^3	(Turton *et al* 2008)
Pump	Reciprocating	3.8696	0.3161	0.1200	Shaft Power, kW	(Turton *et al* 2008)
Compressor	Centrifugal	2.2891	1.3604	-0.1027	Fluid Power, kW	(Turton *et al* 2008)

$C_p = Capital\ cost = \text{Antilog}_{10}(k_1 + k_2 \log_{10} A + k_3 (\log_{10} A)^2$ (Turton *et al* 2008) (3)

Pressure factor

$$F_{p,vessel} = Pressure\ factor = \frac{\frac{(P+1)D}{2(850 - 0.6(P+1))} + 0.00315}{0.0063}$$

Where D= diameter of the vessel in meters, and P= Operating pressure (barg)

Material Factor and Bare Module cost

$C_{bm} = Bare\ Module\ cost = C_p F_{bm} = C_p(B_1 + B_2 F_m F_p)$ (Turton *et al* 2008) (4)

Table 11. Constants for Bare Module Factor used in Eqn. 4

Equipment	Equipment material	Material factor, F_m	B_1	B_2
Process Vessel	Carbon steel	1.0	2.25	1.82

5.1.2.2 Operating Cost

I. Fixed Capital Investment (FCI)
II. Cost of operating Labor (C_{OL})
III. Cost of utilities (C_{UT})
IV. Cost of waste treatment (C_{WT})
V. Cost of Raw materials (C_{RM})

$$Operating\ Cost = C_{RM} + C_{WT} + C_{OL} + 0.1FCI + C_{UT} \quad (5)$$

a. Cost of Operating Labor

A single operator works on the average 49 weeks a year (3 weeks times off for vacation and sick leave), five 8-hour shifts a week. [49 weeks/year * 5 shifts/week] = 245 shifts per operator per year.

Operation time = 24 hours/day

This requires (365 days/year * 3 shifts/day) = 1095 operating shifts per year / (245 shifts/operator/year) = 4.5 operators are hired for each operation needed in the plant at any time.

Plant and system operator wage = $26.48/hr. (Turton *et al* 2008)

$$N_{ol} = (6.29 + 31.7P^2 + 0.23N_{op})^{0.25}$$

N_{ol} = Number of operators per shift

P = Number of processing steps involving the handling of particulate solids

N_{op}= Number of non-particulate processing steps

In this case study, there are no particulate solids processing units, and only the adsorber is considered for non-particulate processing equipment.

N_{op}= 1

$$N_{ol} = (6.29 + 31.70^2 + 0.23 * 1)^{0.25}$$

$$N_{ol} = 1.597$$

Operating Labor = Number of operators hired per operation * Number of operator per shift, N_{ol}

Operating Labor = 4.5 * 1.597 = 7.16 ≈ 7

Labor Cost = Operating Labor * Wage * 2000(hour/year) = 7*26.48*2000= $370,720 per year

b. Cost of Utility/ Regeneration Cost

Cost of steam from boiler (Low pressure (5 barg, 160 °C)) = $13.28/GJ (Turton *et al* 2008)

Energy required for regeneration = (Mass of adsorbent * Specific heat capacity * Temperature)/ Heating efficiency

Where Heating Efficiency = 50%

c. Cost of Raw Materials

1. 3-Aminopropyltriethoxysilane APTES = $5.0 per kg (Alibaba 2019)
2. SBA-15 = $1,690 per 1000 kg (Alibaba 2019)

5.2 Excel Economic Model Outlook

Volumetric Flowrate	1000	SCFM	1714.285	Nm3/hr
Adsorption Capacity	0.85	mmol/g	37.4085	mg/g
Regeneration Capacity	2000	Cycle		
Mass of adsorbent required	71045	Kg		
Adsorbent Cost	$ 147,000.00			
	$ 2.07	per Kg		
Volume of Process Vessel	530.4603549	m3		
Process Vessel Height	40.719	m		
Process Vessel Diameter	4.072	m		
Operating Pressure	1	bar		
Compressor Capaciy	10	kW		
Vessel Purchase Cost	$ 329,000	per unit		
Vessel Bare Module Cost	$ 1,494,000	per unit		
Compressor Purchase Cost	$ 4,000	per unit		
Compressor Bare Module Cost	$ 10,000.00	per unit		
Adsorption temperature	25	Degree		
Regeneration Temperature	100	Degree		
Steam unit cost	13.28	$/GJ		
Energy Required	9.8	GJ		
Regneration Cycle	12	per day		
Regeneration Cost	$ 571,000	Per year		
Regeneration Cost	$ 8.04	Per Kg/Yr		

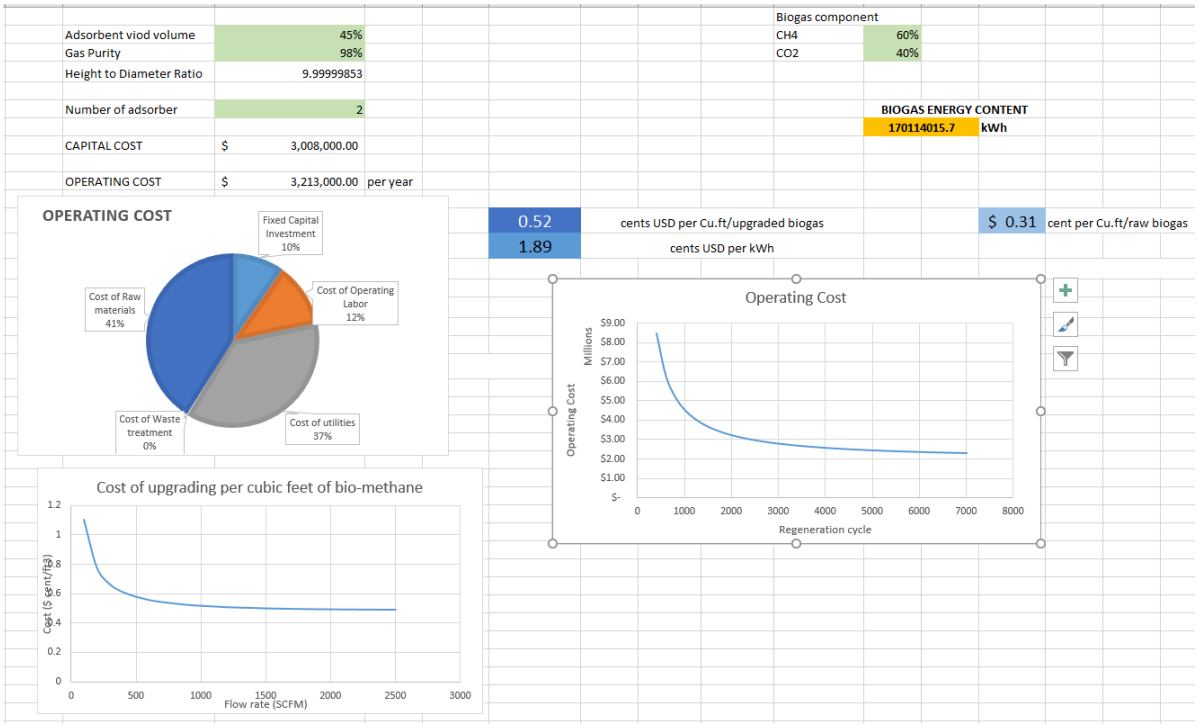

Figure 25. Excel economic model outlook

5.3 Results and Discussion

The simulation of biogas upgrading using Supported Amine Sorbent (SAS) was performed. Two adsorbing columns of capacity, 530 m^3, and packing height of 40 m was estimated. The capital cost was estimated to be 3 million USD as summarized in Table 12. Table 13 provides a breakdown of the plant operating cost estimation. Approximately 3.2 million USD is required annually. As shown in Figure 26, the contributors to the operating cost of the process are the cost of raw materials, and the cost of utilities or regeneration costs are 41 and 37%, respectively. The cost of the raw materials includes the cost of intermediary adsorbent preparation materials and the cost of preparation. This process is an improvement compared with other technology such as amine scrubbing with high regeneration energy consumption.

Table 12. Capital Cost

Equipment	Purchase Cost per unit	Bare Module Cost per unit	Total Cost
Process Vessel	$ 329,000	$ 1,494,000	$ 2,988,000
Compressor	$ 4,000	$ 10,000.00	$ 20,000
Capital Cost			$ 3,008,000

Table 13. Operating Cost Distribution

Fixed Capital Investment	$300,800
Cost of Operating Labor	$370,700
Cost of utilities	$1,142,000
Cost of Waste treatment	$6,600
Cost of Raw materials	$1,270,000
Total Operating Cost per Annum	$3,090,000

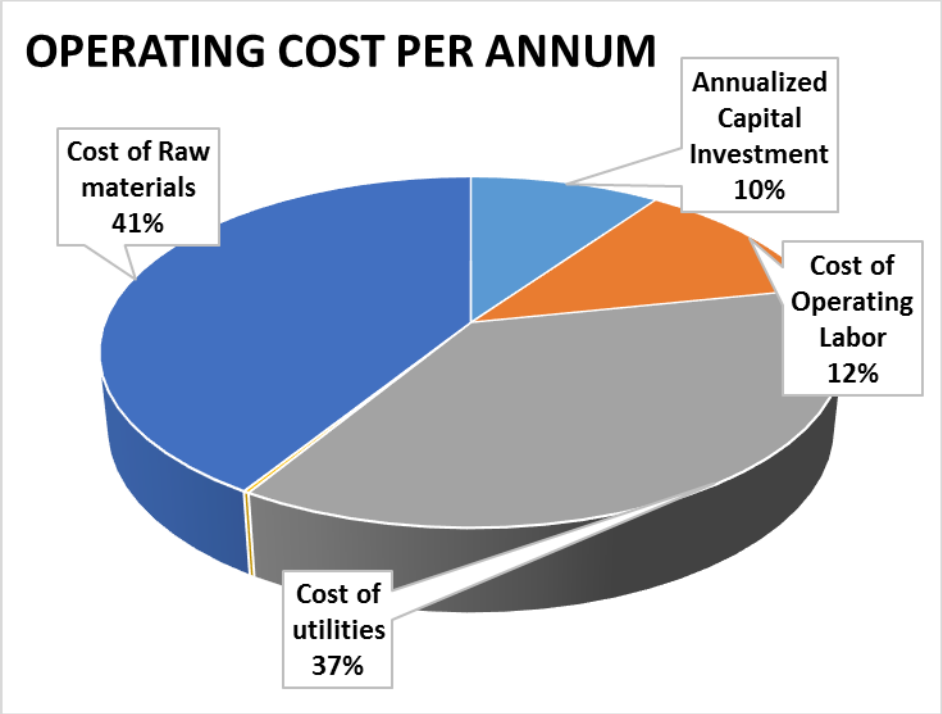

Figure 26. Distribution of operating cost of the SAS system

5.3.1 Sensitivity Analysis

The economic evaluation of scale for biogas upgrading is presented in Figure 27. The scale used is 100 to 2500 SCFM. The overall plant operation cost reduces significantly with an increase in plant capacity. High plant capacity should be desired to achieve the economic viability of the process. A flowrate of 400 SCFM to 1000 SCFM must be achieved to obtain at 0.5 – 0.6 cents $ per cubic feet of bio-methane. This figure evaluates the upgraded biogas price with scale; this allows for plants to judge if biogas upgrading is economically viable.

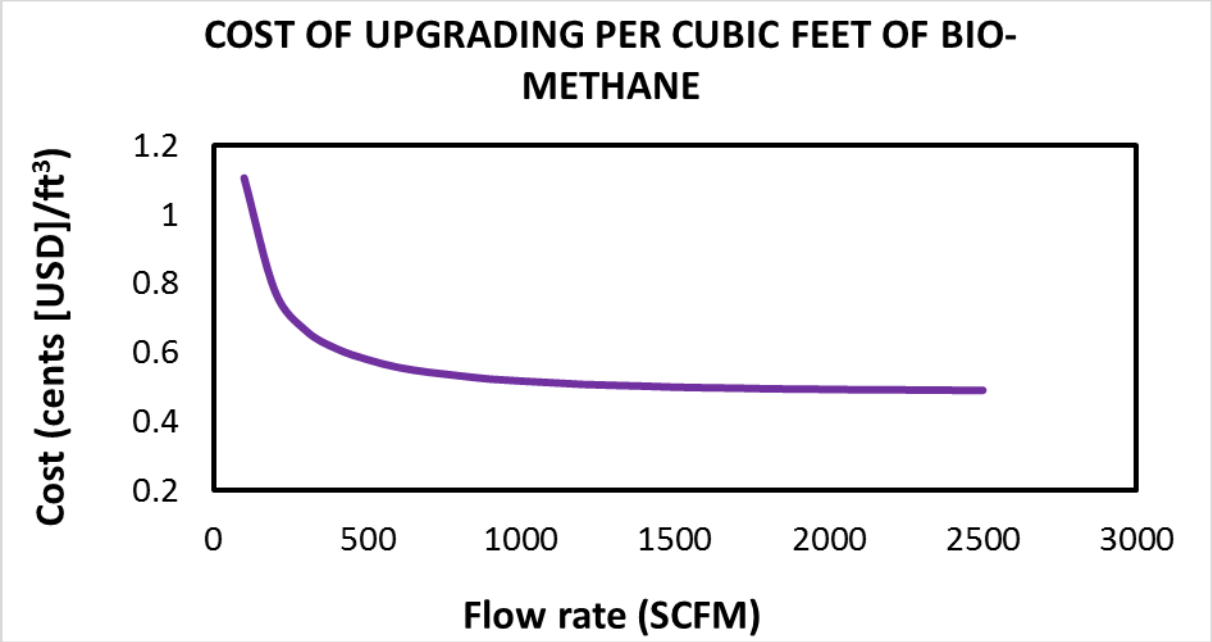

Figure 27. Cost of biogas upgrading at different SAS plant scales

Figure 28 demonstrated the impact of sorbent regenerability on the plant's operational cost. The before deactivating until 4000 cycles. The sorbent must be able to be regenerable for at least 2000 cycles to stay below the 3 million dollars operating cost.

Figure 28. Impact of adsorbent regeneration cycles allowed on overall process operating cost

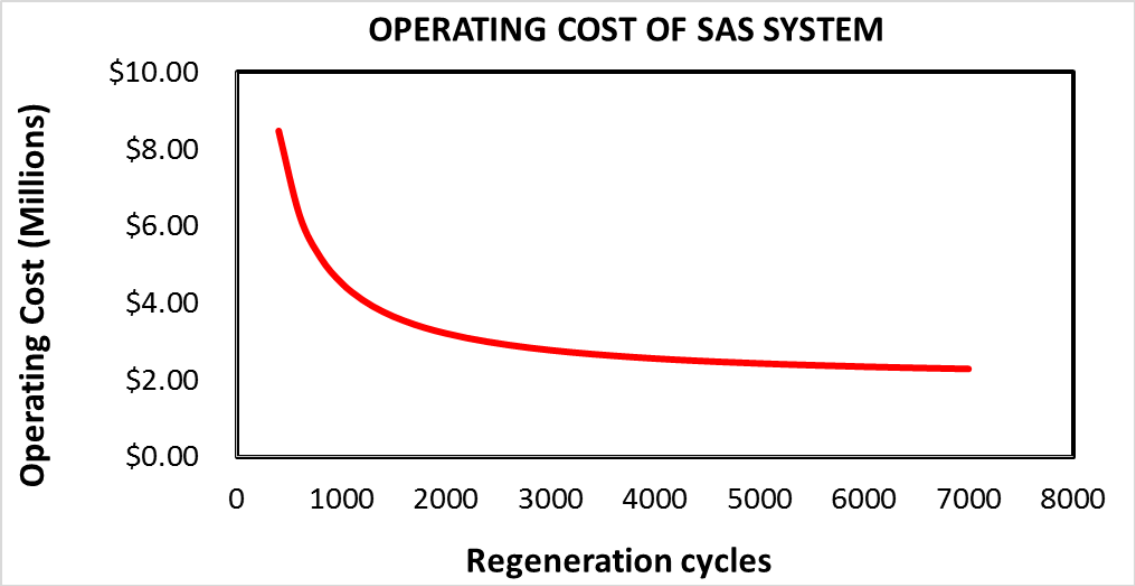

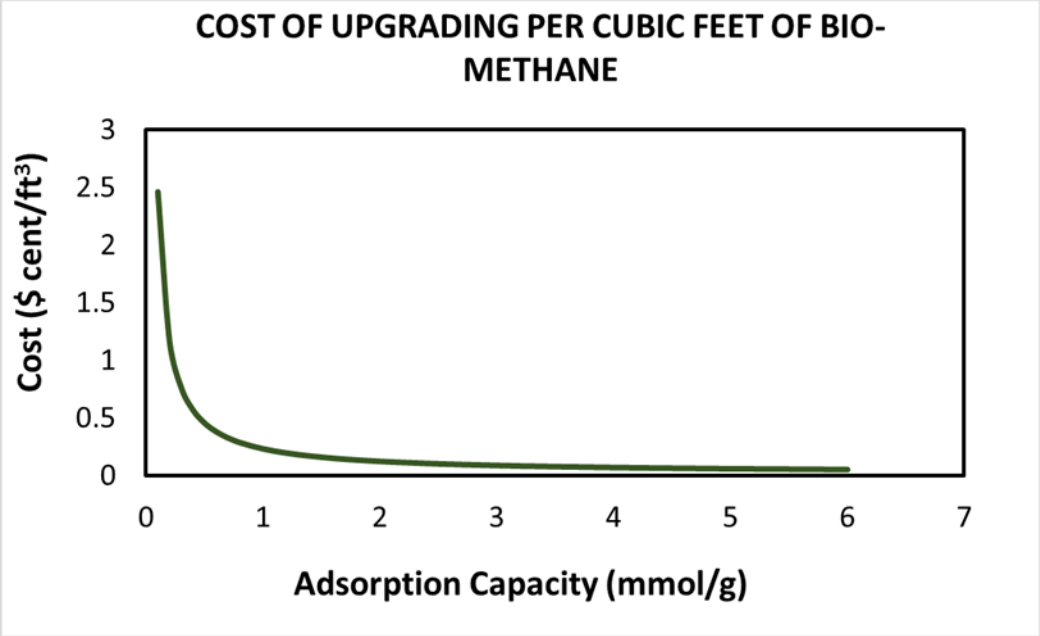

Figure 29. Impact of sorbent adsorption capacity on the cost of upgrading

The impact of sorbent adsorption capacity was also evaluated (Figure 29). The adsorption capacity is required at 1.0 $mmol_{CO2}/g_{ads}$ for the cost of the upgrading of biogas to stay below 0.5 cents $. The cost of upgrading is similar at the adsorption capacity of 3.0 $mmol_{CO2}/g_{ads}$ and greater. This shows that sorbent stability has more impact on the cost of upgrading than the adsorption capacity. The ideal adsorbent at present conditions should have an adsorption capacity upward of 3.0 $mmol_{CO2}/g_{ads}$ and regenerability cycles of 4000.

5.3.2 Comparison with Existing Technologies

The capital cost data obtained from the design project is compared with other existing technologies and for all capacities of plant considered. The SAS system has the lowest fixed capital investment as shown in Figure 30. The existing biogas upgrading technologies considered include Pressure Swing Adsorbent (PSA), High-Pressure Water Scrubbing (HPWS), Chemical scrubbing Process (CSP), and Membrane Separation (Khan *et al* 2017). The capital cost per plant capacity (m^3/hr) decreased with increasing capacity until the capacity of 600 m^3/hr, as it increases with increasing plant capacity.

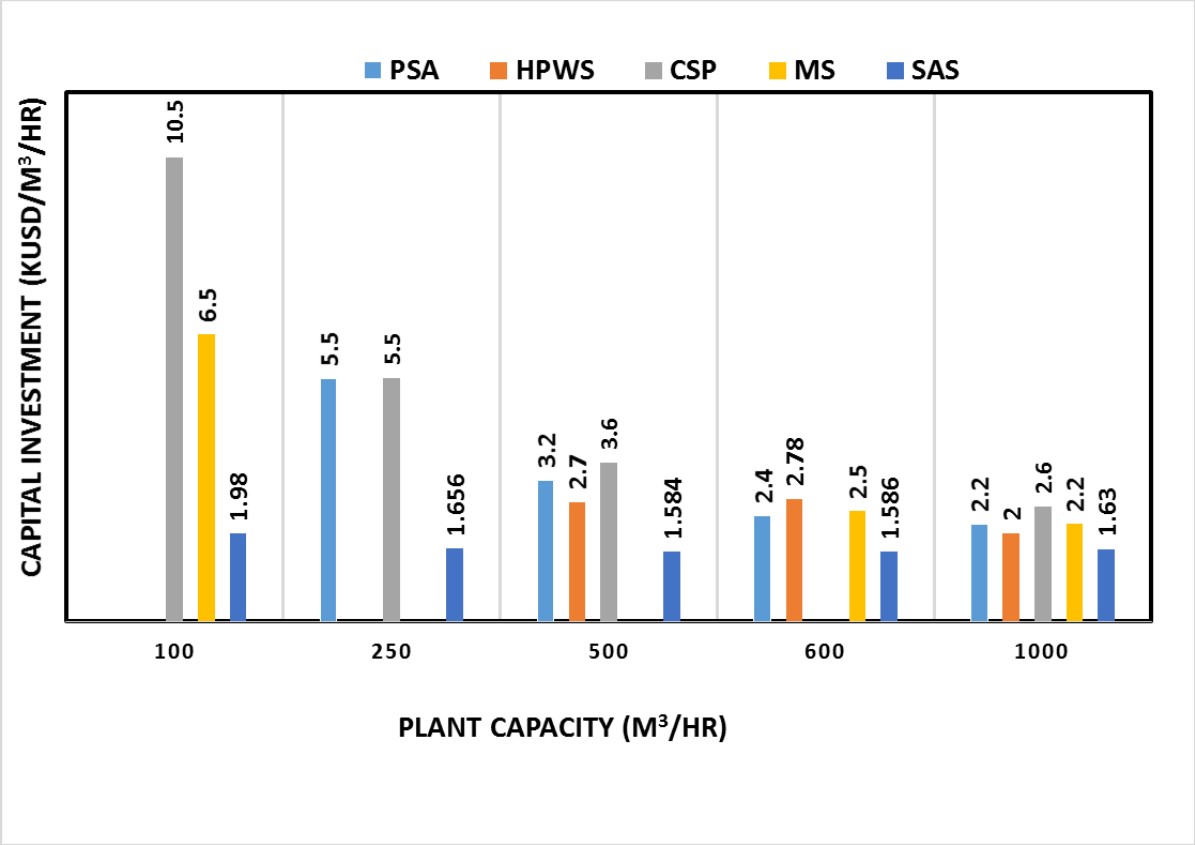

Figure 30. Capital investment cost of different upgrading technologies (Khan et al 2017).

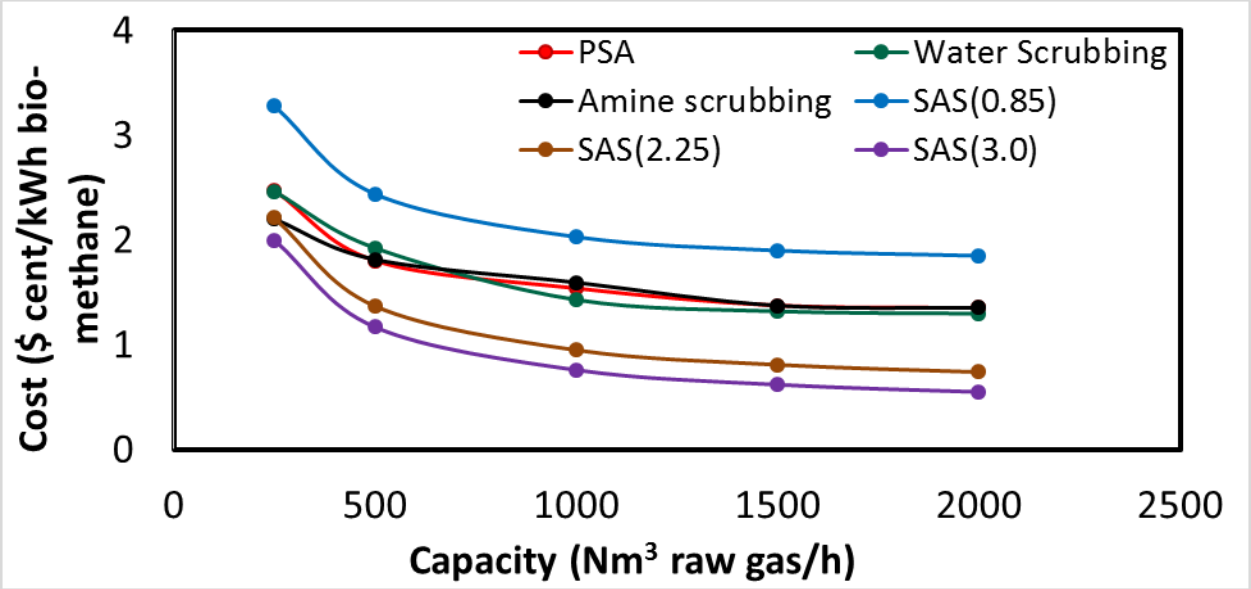

Figure 31. Cost for biogas upgrading for methane (PSA, Water scrubbing and Amine scrubbing data adapted from Petersson and Wellinger, 2009)

The cost as a function of biogas scale for the different technologies and different scales for the upgrading technologies is shown in Figure 31. The graph shows that for all for the processes considered, the cost decreases when the capacity of the biogas plants increases. SAS technology has the lowest cost of upgrading per kWh of bio-methane at all plant capacities and also decreases with increasing adsorption in parentheses. The data for PSA, water scrubbing, and amine scrubbing are adapted from (Petersson and Wellinger 2009).

5.3.3 Comparison to Natural Gas

Natural gas market value averaged at $3.48 per 1000 cubic feet of natural gas from October 2018 to September 2019, ranging from $ 4.93 to $ 2.03 per 1000 cubic feet of natural gas (Hub 2019). The current price pegged at $2.25 per 1000 cubic feet of natural gas. The simulation result indicated that the price of bio-methane produced from a SAS system is $5.2 per 1000 cubic feet of methane. However, at the adsorption capacity of 3.0 $mmol_{CO2}/g_{ads}$ and regeneration cycle of 4000, the price is estimated to reduce drastically to $1.62 per 1000 cubic feet of methane. Although methane price cannot compete currently with natural gas without renewable energy credit, this result demonstrated that with improvements in SAS technology and the availability of renewable energy credit, methane produced could be economically viable in comparison with natural gas.

5.4 Summary

Biogas is a renewable fuel that can be used directly as fuel for combustion engines, gas turbines, fuel-cells, or feed into the natural gas grid, provided impurities (CO_2, H_2S, and H_2O) are removed according to specifications prior to grid injection. Compared to conventional technologies, amine-functionalized silica sorbents seem attractive for their high adsorption capacities, high selectivity for CO_2 and fast uptake rate. In this study, techno-economic sensitivity analyses for the conceptual design of a system for CO_2 separation from biogas with amine-functionalized silica sorbents were completed. The performance is compared to current biogas upgrading technologies such as pressure swing adsorption, water scrubbing, amine scrubbing, and membrane separation. As the basis of this study, 1000 SCFM of raw biogas with 40% volume of CO_2 is to be upgraded to a gas product containing less than 3% of CO_2 as required by national natural gas grid guideline. The process and economic studies show that the amine-functionalized sorbent does not only provide the technical capacity to satisfy the requirement on gas quality, but it also provides a reduction in energy consumption in addition to cost minimization. To achieve process economic viability, the sorbent used for the process is required to have an adsorption capacity of 3.0 $mmol_{CO2}/g_{ads}$ and regenerability of 4000 cycles. The cost of upgrading using the amine-functionalized silica decrease with increasing plant capacity and it is projected to require the least capital and operating investment when compared to current biogas upgrading technologies.

6. CONCLUSIONS AND FUTURE WORK

In this work, various loadings of APTES modified SBA-15 were prepared and tested to study the effect of loading on CO_2 separation. The experiments were conducted at room temperature and 1 atm pressure. Desorption experiments were conducted at 100 °C. The adsorption capacity of 0.85 mmol/g is achieved by the adsorbent at its maximum loading of 26 wt% APTES. The adsorbent performance in the presence of water was studied and it was seen that the adsorption capacity of the absorbents decreased to 0.72 mmol/g. However, during the five regeneration cycles conducted, this capacity remained constant. The sample was tested with real LFG. The adsorption capacity of the LFG decreased by almost 30%. However, regeneration studies for up to 5 cycles showed consistent adsorption capacity.

The potential of the SASs as part of a CO_2 removal system for biogas upgrading was evaluated with the process and economic studies. SAS technology provides the technical capacity to satisfy the requirement of gas quality. It also provides a reduction in energy consumption in addition to cost minimization. The sensitivity study shows that the process is strongly dependent on plant capacity, the number of regeneration cycles allowed, and the adsorption capacity of the silica sorbent used. The stability of the sorbent is the most important property, as it controls the lifespan of the material. The sorbent is recommended to have an adsorption capacity of 3.0 $mmol_{CO2}/g_{ads}$ and regenerability of 4000 cycles to achieve economic viability and feasibility.

From the experimental and techno-economic results, it can be concluded that amine-modified silica has a high potential for removing CO_2 from LFG along with water in the same step process. However, more verification should be completed before it can be actually used in a biogas upgrading plant. Future studies should include examining: 1) Effect of adsorption/desorption temperature to see if adsorbent working capacity improves, 2) CO_2 adsorption for higher number of cycles (above 10) as H_2S in LFG may not be adequately desorbed after a large number of cycles, 3) Effect of the individual impurities present in LFG on CO_2 adsorption capacity, and finally 4) Synthesize and test different amine functionalization for LFG purification.

REFERENCES

AEBIOM. A Biogas Road Map for Europe. European Biomass Association, 2012.

Alibaba. 2019 [cited for costing of selected chemicals at scale] https://www.alibaba.com/.

Awe, O.W., Zhao, Y., Nzihou, A., Minh, D.P., and Lyczko, N. "A Review of Biogas Utilisation, Purification and Upgrading Technologies," Waste and Biomass Valorization. 8: 267-83 (2017).

AZoM. Properties:Silica-Silicon Dioxide (SiO_2). 2019 [cited 2019 10/02]; Available from: www.azom.com/properties.aspx?ArticleID=1114

Bauer, F., Hulteberg, C., Persson, T., and Tamm, D. Biogas upgrading – Review of commercial technologies. Sweden: SGC Rapport, 2013.

Belmabkhout, Y., De Weireld, G., and Sayari, A. "Amine-Bearing Mesoporous Silica for CO_2 and H_2S Removal from Natural Gas and Biogas," Langmuir. 25: 13275-8 (2009a).

Belmabkhout, Y., and Sayari, A. "Adsorption of CO_2 from dry gases on MCM-41 silica at ambient temperature and high pressure. 2: Adsorption of CO_2/N_2, CO_2/CH_4 and CO_2/H_2 binary mixtures," Chemical Engineering Science. 64: 3729-35 (2009).

Belmabkhout, Y., Serna-Guerrero, R., and Sayari, A. "Adsorption of CO_2-Containing Gas Mixtures over Amine-Bearing Pore-Expanded MCM-41 Silica: Application for Gas Purification," Industrial & Engineering Chemistry Research. 49: 359-65 (2010a).

Belmabkhout, Y., Serna-Guerrero, R., and Sayari, A. "Adsorption of CO_2 from dry gases on MCM-41 silica at ambient temperature and high pressure. 1: Pure CO_2 adsorption," Chemical Engineering Science. 64: 3721-8 (2009b).

Belmabkhout, Y., Serna-Guerrero, R., and Sayari, A. "Amine-bearing mesoporous silica for CO_2 removal from dry and humid air," Chemical Engineering Science. 65: 3695-8 (2010b).

Börjesson, P., Berglund, M.J.B., and bioenergy "Environmental systems analysis of biogas systems—Part I: Fuel-cycle emissions," 30: 469-85 (2006).

Budzianowski, W.M. "Benefits of biogas upgrading to biomethane by high-pressure reactive solvent scrubbing," Biofuels, Bioproducts and Biorefining. 6: 12-20 (2012).

Cano, L.A., Cagnoli, M.V., Bengoa, J.F., Alvarez, A.M., and Marchetti, S.G. "Effect of the activation atmosphere on the activity of Fe catalysts supported on SBA-15 in the Fischer–Tropsch Synthesis," Journal of Catalysis. 278: 310-20 (2011).

Chang, F.-Y., Chao, K.-J., Cheng, H.-H., and Tan, C.-S. "Adsorption of CO_2 onto amine-grafted mesoporous silicas," Separation and Purification Technology. 70: 87-95 (2009).

Chaudhary, V., and Sharma, S. "An overview of ordered mesoporous material SBA-15: synthesis, functionalization and application in oxidation reactions," Journal of Porous Materials. 24: 741-9 (2017).

Choi, S., H. Drese, J., Eisenberger, P., and W. Jones, C. A New Paradigm of Anthropogenic CO_2 Reduction: Adsorptive Fixation of CO_2 From the Ambient Air as a

Carbon Negative Technology, Aiche Annual Meeting (2009) https://www.aiche.org/conferences/aiche-annual-meeting/2009/proceeding/paper/679e-new-paradigm-anthropogenic-co2-reduction-adsorptive-fixation-co2-ambient-air-carbon-negative.

Danckwerts, P.V. "The reaction of CO_2 with ethanolamines," Chemical Engineering Science. 34: 443-6 (1979).

Eisenberger, P.M., Cohen, R.W., Chichilnisky, G., Eisenberger, N.M., Chance, R.R., and Jones, C.W. "Global Warming and Carbon-Negative Technology: Prospects for a Lower-Cost Route to a Lower-Risk Atmosphere," Energy & Environment. 20: 973-84 (2009).

EPA "Advancing Sustainable Materials Management: 2014 Fact Sheet, https://www.epa.gov/sites/production/files/2016-11/documents/2014_smmfactsheet_508.pdf," (2016).

EPA. Project and Landfill Data by State: Landfill Methane Outreach Program (LMOP); 2019.

F. Bauer, C.H., T. Persson, D. Tamm. Biogas upgrading—review of commercial technologies. SGC Rapport 2013 [cited 6/21/2019]; Available from: http://www.sgc.se/ckfinder/userfiles/files/SGC270.pdf

Fauth, D.J., Gray, M.L., Pennline, H.W., Krutka, H.M., Sjostrom, S., and Ault, A.M. "Investigation of Porous Silica Supported Mixed-Amine Sorbents for Post-Combustion CO_2 Capture," Energy & Fuel. 26: 2483-96 (2012).

Gatti, G., Vittoni, C., Costenaro, D., Paul, G., Mangano, E., Brandani, S., Marchese, L., and Bisio, C. "The influence of particle size of amino-functionalized MCM-41 silicas on CO_2 adsorption," Physical Chemistry Chemical Physics. 19: 29449-60 (2017).

Gopalakrishnan, U. Carbon Dioxide Adsorption Using Solid Amine Sorbents. Tampa: M.S. Thesis, University of South Florida; 2019.

Hjuler, K., and Aryal, N. Review of Biogas Upgrading FutureGas project, WP1. Project report. Denmark: Dansk Gasteknisk Center; 2017 09/20/2017. Report No.: 978-87-7795-403-0.

Hoyer, K., Hulteberg, C., Svensson, M., Jernberg, J., and Nørregård, Ø. Biogas Upgrading - Technical Review. 2016 [cited 6/21/2019]; Available from: http://vav.griffel.net/filer/C_Energiforsk2016-275.pdf

Hub, H. Natural Gas Price Today. 2019 [cited 2019 10/03]; Available from: https://markets.businessinsider.com/commodities/natural-gas-price

Jang, W.-J., Kim, H.-M., Shim, J.-O., Yoo, S.-Y., Jeon, K.-W., Na, H.-S., Lee, Y.-L., Jeong, D.-W., Bae, J.W., Nah, I.W., and Roh, H.-S. "Key properties of Ni-MgO-CeO_2, Ni-MgO-ZrO_2, and Ni-MgO-$Ce_{(1-x)}Zr_{(x)}O_2$ catalysts for the reforming of methane with carbon dioxide," Green Chemistry. 20: 1621-33 (2018).

Kadam, R., and Panwar, N.L. "Recent advancement in biogas enrichment and its applications," Renewable and Sustainable Energy Reviews. 73: 892-903 (2017).

Kent, R.A. Conversion of Landfill Gas to Liquid Hydrocarbon Fuels: Design and Feasibility Study [M.S. Thesis]: University of South Florida; 2016.

Khan, I.U., Othman, M.H.D., Hashim, H., Matsuura, T., Ismail, A., Rezaei-DashtArzhandi, M., and Azelee, I.W. "Biogas as a renewable energy fuel–A review of biogas upgrading, utilisation and storage," Energy Conversion and Management. 150: 277-94 (2017).

Kishor, R., and Ghoshal, A.K. "Amine-Modified Mesoporous Silica for CO_2 Adsorption: The Role of Structural Parameters," Industrial & Engineering Chemistry Research. 56: 6078-87 (2017).

Kishor, R., and Ghoshal, A.K. "APTES grafted ordered mesoporous silica KIT-6 for CO_2 adsorption," Chemical Engineering Journal. 262: 882-90 (2015).

Kumar, R., Barakat, M.A., Daza, Y.A., Woodcock, H.L., and Kuhn, J.N. "EDTA functionalized silica for removal of Cu(II), Zn(II) and Ni(II) from aqueous solution," Journal of Colloid and Interface Science. 408: 200-5 (2013).

Lara, Y., Romeo, L.M., Lisbona, P., Espatolero, S., and Escudero, A.I. "Efficiency and Energy Analysis of Power Plants with Amine-Impregnated Solid Sorbents CO_2 Capture," Energy Technology. 6: 1649-59 (2018).

Lee, U., Han, J., and Wang, M. "Evaluation of landfill gas emissions from municipal solid waste landfills for the life-cycle analysis of waste-to-energy pathways," Journal of Cleaner Production. 166: 335-42 (2017).

Liu, X., Zhai, X., Liu, D., and Sun, Y. "Different CO_2 absorbents-modified SBA-15 sorbent for highly selective CO_2 capture," Chemical Physics Letters. 676: 53-7 (2017).

LMOP "Project and Landfill Data by State," United States Environmental Protection Agency, https://wwwepagov/lmop/project-and-landfill-data-state. (2019).

Mafra, L., Čendak, T., Schneider, S., Wiper, P., Pires, J., Gomes, J., and Pinto, M. "Amine functionalized porous silica for CO_2/CH_4 separation by adsorption: Which amine and why" Chemical Engineering Journal. 336: 612-21 (2017).

Mokhatab, S., Poe, W.A., and Mak, J.Y. Chapter 4 - Basic Concepts of Natural Gas Processing. In: Mokhatab S, Poe WA, Mak JY, eds. Handbook of Natural Gas Transmission and Processing (Fourth Edition): Gulf Professional Publishing, 2019:177-89.

Mokhatab, S., Poe, W.A., and Mak, J.Y. Handbook of natural gas transmission and processing: principles and practices: Gulf Professional Publishing, 2018.

Petersson, A., and Wellinger, A. Biogas upgrading technologies-Developments and innovations 2009. IEA Bioenergy Task 37 2009 [cited 2012 05.03.2012]; Available from: http://www.ieabiogas.net/_download/publi-task37/upgrading_rz_low_final.pdf

Quan, W., Wang, X., and Song, C. "Selective Removal of H_2S from Biogas Using Solid Amine-Based “Molecular Basket” Sorbent," Energy & Fuels. 31: 9517-28 (2017).

Sahota, S., Shah, G., Ghosh, P., Kapoor, R., Sengupta, S., Singh, P., Vijay, V., Sahay, A., Vijay, V.K., and Thakur, I.S. "Review of trends in biogas upgradation technologies and future perspectives," Bioresource Technology Reports. 1: 79-88 (2018).

Scarlat, N., Dallemand, J.-F., and Fahl, F. "Biogas: Developments and perspectives in Europe," Renewable Energy. 129: 457-72 (2018).

Scarlat, N., Dallemand, J.-F., Monforti-Ferrario, F., Banja, M., and Motola, V. "Renewable energy policy framework and bioenergy contribution in the European Union – An overview from National Renewable Energy Action Plans and Progress Reports," Renewable and Sustainable Energy Reviews. 51: 969-85 (2015).

Shi, Y., Liu, Q., and He, Y. CO_2 Capture Using Solid Sorbents. Handbook of Climate Change Mitigation and Adaptation, Second Edition. Switzerland: Springer International Publishing, 2017:2349-404.

Sun, Q., Li, H., Yan, J., Liu, L., Yu, Z., and Yu, X. "Selection of appropriate biogas upgrading technology-a review of biogas cleaning, upgrading and utilisation," Renewable and Sustainable Energy Reviews. 51: 521-32 (2015).

Sutanto, S., Dijkstra, J., Pieterse, J., Boon, J., Hauwert, P., and Brilman, D. "CO_2 removal from biogas with supported amine sorbents: First technical evaluation based on experimental data," Separation and Purification Technology. 184: 12-25 (2017a).

Sutanto, S., Dijkstra, J.W., Pieterse, J.A.Z., Boon, J., Hauwert, P., and Brilman, D.W.F. "CO_2 removal from biogas with supported amine sorbents: First technical evaluation

based on experimental data," Separation and Purification Technology. 184: 12-25 (2017b).

Teng, W., Wu, Z., Feng, D., Fan, J., Wang, J., Wei, H., Song, M., and Zhao, D. "Rapid and Efficient Removal of Microcystins by Ordered Mesoporous Silica," Environmental Science & Technology. 47: 8633-41 (2013).

Turton, R., Bailie, R.C., Whiting, W.B., and Shaeiwitz, J.A. Analysis, synthesis and design of chemical processes: Pearson Education, 2008.

Ullah Khan, I., Hafiz Dzarfan Othman, M., Hashim, H., Matsuura, T., Ismail, A.F., Rezaei-DashtArzhandi, M., and Wan Azelee, I. "Biogas as a renewable energy fuel – A review of biogas upgrading, utilisation and storage," Energy Conversion and Management. 150: 277-94 (2017).

Walas, S.M. Chemical process equipment; selection and design; 1988.

Wang, X., Guo, Q., Zhao, J., and Chen, L. "Mixed amine-modified MCM-41 sorbents for CO2 capture," International Journal of Greenhouse Gas Control. 37: 90-8 (2015).

Warren, K.E.H. A techno-economic comparison of biogas upgrading technologies in Europe [Master's Thesis]: University of Jyväskylä; 2012.

Wikipedia. Carbon dioxide. 2013 [cited 2019 10/02]; Available from: https://en.wikipedia.org/wiki/Carbon_dioxide

Yang, L., Ge, X., Wan, C., Yu, F., and Li, Y. "Progress and perspectives in converting biogas to transportation fuels," Renewable and Sustainable Energy Reviews. 40: 1133-52 (2014).

Zhao, X., Naqi, A., Walker, D.M., Roberge, T., Kastelic, M., Joseph, B., and Kuhn, J.N. "Conversion of landfill gas to liquid fuels through a TriFTS (tri-reforming and Fischer–Tropsch synthesis) process: a feasibility study," Sustainable Energy & Fuels. 3: 539-49 (2019).

Zhou, K., Chaemchuen, S., and Verpoort, F. "Alternative materials in technologies for Biogas upgrading via CO_2 capture," Renewable and Sustainable Energy Reviews. 79: 1414-41 (2017).

Appendices

Appendix A: EDTA Functionalized SBA-15

Synthesis of the adsorbent was done similar to literature. To study the CO_2 adsorption capacity of the sample, 50% CO_2/He was flown through 80 mg of EDTA-SBA15 for 30 min followed by the desorption test at 100 °C. A total flow rate to 30 sccm was used. Signals were allowed to stabilize before both steps. Before the experiment the sample was dried at 100 °C. It showed an adsorption capacity of 0.0081 mmol/g.

Appendix B: Weight Loading Calculation from Calcination Experiment

Table B1: Weight loading calculation from calcination experiment of 26wt%APTES.

$C_9H_{23}NO_3Si$ molar mass	221.372	g/mol
Weight of adsorbent	1	g
Weight after drying	0.9536	g
Weight after calcination	0.7068	g
APTES loading (per gram adsorbent)	26	g

Appendix C: Adsorption Capacity Calculation

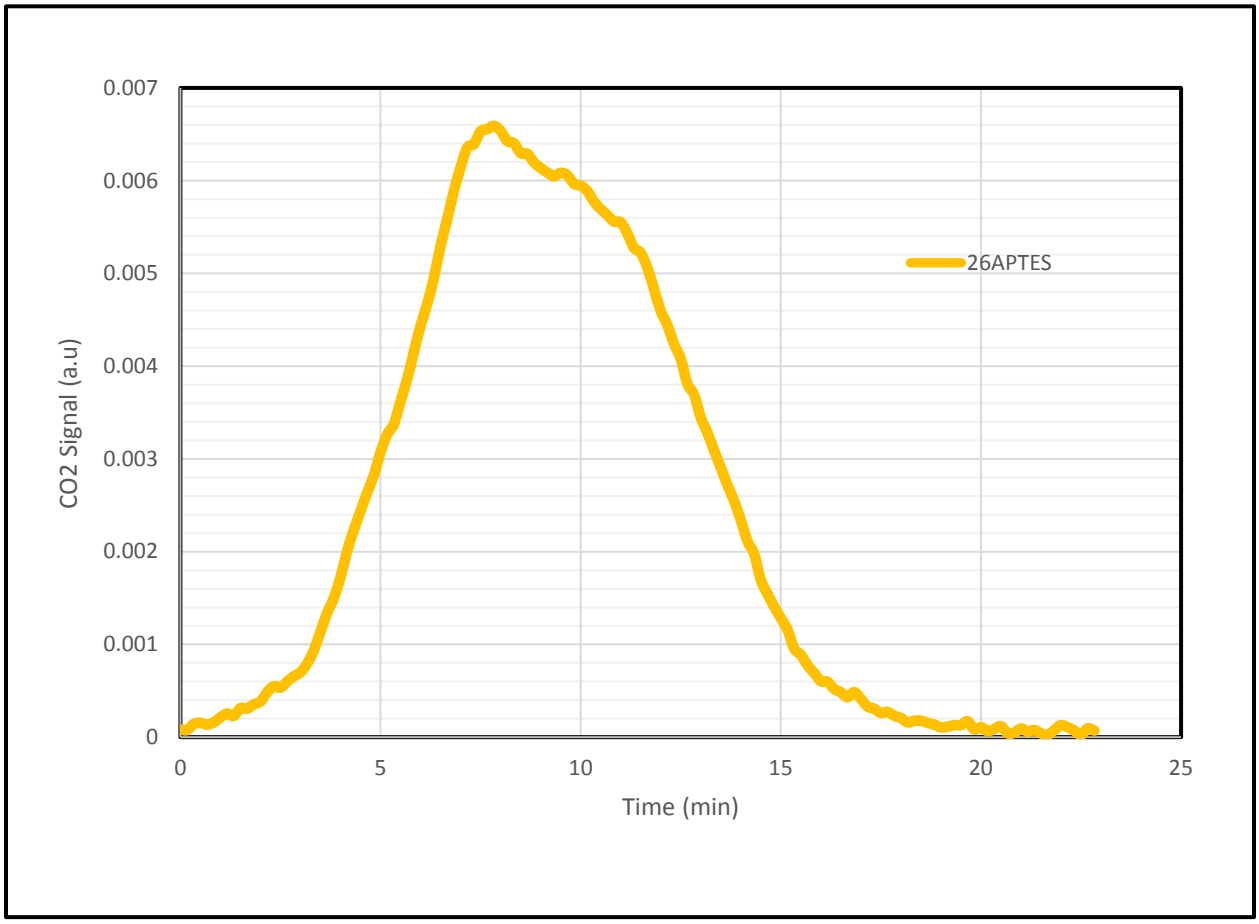

Figure C1: CO_2 Adsorption signal after desorption step of 26wt%APTES

Table C1: Adsorption capacity calculation of 26wt%APTES

Density of CO_2	0.001977	g/cm^3
Molar Mass of CO_2	44.01	g/mol
Adsorbent amount	0.08	g
Volume of CO_2 adsorbed	1.52	cm^3
Mass of CO_2 adsorbed	0.003	g
Moles of CO_2 adsorbed	0.068	mmol
Adsorption capacity of per g of adsorbent	0.85	mmol

Appendix D: Water Flow Rate Calculation

Vapor pressure was determined using Antoine equation;

$$log_{10}^{p} = A - \frac{B}{(C + T)}$$

- p (mm Hg) = Vapor pressure
- A,B,C = Constants
- T (°C) = Temperature

Table D1: Constants for Antoine equation

Temperature	(0-60) °C
A	8.10765
B	1750.286
C	235
T	32 °C

Table D2: Water flow rate calculation

Partial pressure of water	0.05	bar
Total pressure	1.01	bar
Mole fraction of vapor	0.05	
Mole fraction of He	0.95	
Helium flow rate	4	sccm
Water vapor flow rate	0.2	sccm

Appendix E: Weight Percent Calculation from TPO Data

Table E1: Weight percent calculation from TPO data for 26wt%APTES

Molar mass of APTES, $C_9H_{23}NO_3Si$	221.37	g/mol
Density of CO_2	0.001977	g/cm^3
Molar Mass of CO_2	44.01	g/mol
Density of CO	0.00196	g/cm^3
Molar Mass of CO	28.01	g/mol
Moles of C from signal	0.951	mmol
Moles of APTES loaded	0.106	mmol
Mass of APTES loaded	0.023	g
Weight percent of APTES in sample	27.53	wt%

Appendix F: Relative Humidity Calculation

Table F1: Relative humidity sample calculation

CH_4	37.5	mol%
CO_2	37.5	mol%
H_2O	4.1	mol%
He	21	mol%
Total Pressure	1	bar
Saturation Pressure	0.16	bar
Water vapor pressure	0.04	bar
Relative humidity	25	R.H.

Appendix G: Repeated Experiment Data

CO_2 adsorption experiment was repeated with 12wt%APTES was repeated to get the adsorption capacity. This was done in order to ensure repeatability of the experiment. The data is summarized in Table G1.

Table G1: Repeatability study of 12wt%APTES

12wt%APTES	**CO_2 adsorption capacity mmol/g**
Study 1	0.07
Study 2	0.08